# Semi-inclusive deep-inelastic scattering on a polarized spin-1 target. I. Cross section and spin observables

W. Cosyn [1,*] and C. Weiss [2,†]
[1] *Department of Physics, Florida International University, Miami, Florida 33199, USA*
[2] *Theory Center, Jefferson Lab, Newport News, Virginia 23606, USA*

(Received 13 April 2026; revised 31 May 2026; accepted 18 June 2026; published 3 August 2026)

We develop the theoretical framework for semi-inclusive deep-inelastic scattering on a polarized spin-1 target and apply it to scattering on the polarized deuteron with spectator nucleon tagging. In Part I (this article) we present the general form of the semi-inclusive cross section and polarization observables for the spin-1 target. A relativistically covariant formulation in terms of four-vectors and invariant polarization parameters is employed. The target polarization is described by a spin density matrix with vector and tensor polarization. The spin and azimuthal angle dependence of the semi-inclusive cross section is derived and parametrized in terms of invariant structure functions. To validate the result, the structure functions are expressed as photon-target helicity amplitudes with known symmetry properties. The expressions presented here are kinematic (no assumptions about particle production dynamics) and valid in all regions of the deep-inelastic final state (current and target fragmentation regions). In Part II (following article), we consider deep-inelastic scattering on the polarized deuteron with spectator nucleon tagging as a special case of target fragmentation. The semi-inclusive structure functions are computed by separating nuclear and hadronic structure, and the polarization observables are explored as functions of the tagged nucleon momentum.

DOI: 10.1103/cwp5-7c96

## I. INTRODUCTION

This is Part I of a study of semi-inclusive deep-inelastic scattering on a polarized spin-1 target. It presents the general form of the semi-inclusive cross section and polarization observables for the spin-1 target. Part II [1] considers deep-inelastic scattering on the polarized deuteron with spectator nucleon tagging.

Deep-inelastic lepton scattering (DIS) is a principal tool for exploring the structure of hadrons and nuclei and the dynamics of strong interactions at short distances. The momentum transfer $Q^2 \gtrsim 1\ \mathrm{GeV}^2$ resolves structures at transverse distances much smaller than the hadronic size $\approx$1 fm. The energy transfer $\nu \gg 1$ GeV causes hadron production over a wide rapidity interval and separates current and target fragments in the final state. Basic information comes from measurements of the lepton-target differential cross section without specification of the hadronic final state (inclusive DIS). Further information is obtained from measurements of the lepton and target spin dependence (polarized DIS). Even more information becomes available with measurements of single-identified hadrons in the final state (semi-inclusive DIS or SIDIS, unpolarized and polarized). Combinations of these measurements make it possible to probe specific elements of the target structure or the final state.

Most theoretical and experimental efforts in polarized DIS have focused on the spin-1/2 target of the nucleon; see Refs. [2–5] and references therein. Measurements of polarized inclusive DIS on the nucleon probe the polarized quark and gluon distributions in the context of the QCD factorization of the cross section [6–8]. Measurements of polarized SIDIS on the nucleon in the current fragmentation region provide information on the flavor decomposition of the polarized quark distributions and spin-orbit effects in the transverse momentum–dependent (TMD) distribution and fragmentation functions [9]. While several experiments in polarized DIS and SIDIS [10–14] have used the spin-1 deuteron as a target, they have been interpreted in terms of scattering on a polarized neutron (after subtracting the proton), with the role of the deuteron limited to providing the effective polarization of the neutron.

Fewer efforts have been devoted to studying the specific polarization effects arising in DIS on targets with spin $>1/2$. A new aspect of spin-1 targets is the possibility of tensor polarization in addition to vector polarization, giving rise to new structures in the cross section [15,16]. Inclusive DIS on the tensor-polarized deuteron was explored at HERMES [17] and will be studied in dedicated experiments at JLab [18–21]. The theoretical interpretation focuses on nuclear binding effects on the partonic structure at large $x$ ($\gtrsim$0.1) [15,22–24] and on nuclear shadowing dynamics at small $x$ ($\ll$0.1) [25–28]. Recent work has explored SIDIS on spin-1 targets in the

*Contact author: wcosyn@fiu.edu
†Contact author: weiss@jlab.org

*Published by the American Physical Society under the terms of the Creative Commons Attribution 4.0 International license. Further distribution of this work must maintain attribution to the author(s) and the published article's title, journal citation, and DOI. Funded by SCOAP³.*

current fragmentation region and the new TMD distributions arising in this context [29–33]. The tensor polarization gives rise to new spin-orbit effects in SIDIS observables and TMD distributions, making it possible to explore new aspects of partonic structure.

DIS on the deuteron with detection of a "slow" nucleon (with momenta of the order of a few 100 MeV in the nuclear rest frame) is a special case of SIDIS in the target fragmentation region. In the context of QCD factorization, target fragmentation measurements are described by fracture functions, which combine aspects of parton distribution and fragmentation functions and express both target structure and hadronization dynamics [34–36]. In the case of slow nucleon production in deuteron DIS, the dominant production mechanism is the nuclear breakup, and the cross section can be computed on this basis ("spectator nucleon tagging") [15,37]; this approximation is compatible with QCD factorization and amounts to a particular nonperturbative model of the fracture functions [38]. It presents a unique situation where the SIDIS cross section and spin observables can be predicted on the basis of well-known nuclear dynamics, formulated in nucleon degrees of freedom and their interactions. In particular, the tensor-polarized structures and spin-orbit effects unique to spin-1 SIDIS could be explored in spectator nucleon tagging with the polarized deuteron [15,39].

Measurements of DIS on the deuteron with spectator nucleon tagging are performed in fixed-target scattering experiments at Jefferson Lab, using specialized detectors for slow protons or neutrons emerging from the target (BONuS, ALERT, Deeps, BAND, LAD) [40–46]. Measurements of spectator tagging are also planned at the Electron-Ion Collider (EIC), using the far-forward detectors for charged and neutral beam fragments [47,48]. The collider setup offers several advantages for nuclear breakup detection (see Part II [1] for details). Such measurements could also be performed on the polarized deuteron if polarized deuteron beams become available at EIC; see Refs. [49–51] for the technical prospects.

In this work we develop the theoretical framework for SIDIS on a polarized spin-1 target and apply it to scattering on the polarized deuteron with spectator nucleon tagging. The presentation consists of two parts.

In Part I (this article), we derive the general form of the semi-inclusive cross section and polarization observables for the spin-1 target. A relativistically covariant formulation in terms of four-vectors and invariant polarization parameters is employed. The target polarization is described by a covariant spin density matrix with vector and tensor polarization. The spin and azimuthal angle dependence of the semi-inclusive cross section is derived and parametrized in terms of invariant structure functions. The expressions obtained in this part are general (no assumptions about particle production dynamics) and valid in all regions of the deep-inelastic final state (current and target fragmentation regions). They can be used for any kind of SIDIS measurement on a polarized spin-1 target.

In Part II (following article, Ref. [1]), we consider the specific case of DIS on the polarized deuteron with spectator nucleon tagging. The semi-inclusive structure functions are computed by separating nuclear and hadronic structure, and the polarization observables are explored as functions of the tagged nucleon momentum. The findings are interpreted using the paradigm of "selection of nuclear configurations" by the tagged nucleon momentum. The results obtained in this part involve approximations in the separation of nuclear and hadronic structure (light-front quantization, impulse approximation) and empirical parametrizations of the low-energy nuclear structure. They can be used for quantitative analysis and simulations of experiments in DIS on the deuteron with spectator nucleon tagging.

The derivation of the SIDIS cross section for the spin-1 target here follows earlier work for the spin-1/2 target [52–56]. In the spin-1/2 case the target polarization is characterized by three parameters, and the semi-inclusive cross section involves 18 independent structures with a distinctive dependence on the beam and target polarization and the azimuthal angle of the identified hadron. In the spin-1 case, the target polarization involves five additional tensor polarization parameters, and the semi-inclusive cross section exhibits 23 additional structures, some with new azimuthal dependences not found in the spin-1/2 case. When integrating over the identified hadron momentum, four of these semi-inclusive tensor-polarized structures reduce to the well-known inclusive tensor-polarized structures (denoted by $b_1$ to $b_4$) [16]; the others integrate to zero. The spin-1 SIDIS cross section thus has a much richer structure than the spin-1/2 one, providing opportunities to study spin-orbit phenomena and structures not present in the spin-1/2 system. The form of the spin-1 SIDIS cross section was analyzed recently in Ref. [32]. It can also be compared with the form of the exclusive deuteron electrodisintegration cross section obtained in earlier nuclear physics studies [57] (further references are given in Part II [1]).

The definition of the azimuthal angle variables and coordinate system is an important issue in SIDIS phenomenology. For the azimuthal angles of the target polarization and the final-state hadron momentum we follow the Trento convention (see below) [58]. For the coordinate system we choose the direction of the $z$ axis opposite to the virtual photon momentum, along the direction of the target momentum in the center-of-mass frame, which simplifies the construction of target spin states and the use of light-front quantization for target structure; see Part II [1]. The correspondence with other conventions can easily be established.

The article is organized as follows. Section II describes the general setup, including kinematic variables, basis four-vectors, collinear frames, and final-state variables. Section III presents the description of the polarized spin-1 target, including the covariant spin density matrix, invariant polarization parameters, and the tensor and spin quantum number representations of the density matrix. Section IV presents the derivation of the differential cross section, including the hadronic tensor, its decomposition and structure functions, the final form of the spin-1 semi-inclusive cross section including the azimuthal angle and spin dependence (vector and tensor polarization), and the correspondence with the spin-1 inclusive cross section. Section V describes the spin observables in spin-1 SIDIS, including the preparation of target polarization using combinations of pure spin states, the separation of vector and tensor-polarized structures, azimuthal harmonics,

and spin asymmetries. Section VI presents a summary and possible extensions of the present work.

Appendix A summarizes the changes in definitions relative to the earlier work in Ref. [39]. Appendix B describes an alternative derivation of the spin-1 spin density matrix using quantum-mechanical operators. Appendix C discusses the representation of the spin-1 semi-inclusive structure functions as helicity amplitudes, which is useful for validating the number of types of independent structures. Appendix D outlines the extension of the structural decomposition of the cross section to targets of higher spin ($>1$). Appendix E describes the correspondence of our semi-inclusive cross-section parametrization with that of Ref. [32] in the current fragmentation region.

## II. PROCESS AND VARIABLES

### A. Kinematic variables

We consider the scattering of a polarized lepton $e$ on a polarized spin-1 target $A$, with detection of the scattered lepton $e'$ and a specified hadron $h$ in the final state, and no restriction on the rest of the hadronic final state $X$ (semi-inclusive scattering),

$$e(l|\lambda_e) + A(P|S,T) \to e'(l') + X + h(P_h). \tag{2.1}$$

$l$ and $l'$ are the initial and final lepton four-momenta; we neglect the lepton mass. $P$ is the target four-momentum, $P^2 = M^2$, and $P_h$ is the detected hadron four-momentum, $P_h^2 = M_h^2$; we follow the notation of Ref. [54] for the spin-1/2 target. The initial state is characterized by the squared center-of-mass energy, described by the invariant variable

$$s \equiv (l+P)^2. \tag{2.2}$$

The four-momentum transfer to the target is

$$q \equiv l - l', \quad Q^2 \equiv -q^2. \tag{2.3}$$

The hadronic scattering process is characterized by the energy and momentum transfer to the target, described by the invariant scaling variables[1]

$$x_A = \frac{Q^2}{2q\cdot P}, \quad y = \frac{q\cdot P}{l\cdot P}, \tag{2.4}$$

which satisfy $0 < x_A \leqslant 1$ and $0 < y < 1$. The kinematic boundaries in a given setup are determined by the condition

$$Q^2 = x_A y (s - M^2). \tag{2.5}$$

The final state with the identified hadron $h$ is characterized by three additional momentum variables, which are defined using a specific reference frame (see below).

The initial lepton in the scattering process Eq. (2.1) is in a pure spin state described by the helicity $\lambda_e = \pm 1/2$. The spin-1 target $A$ is in a mixed spin state described by a density matrix, parametrized by the vector and tensor polarization parameters, $S$ and $T$; its definition and properties are described in Sec. III.

[1] $x_A$ denotes the Bjorken scaling variable for the target $A$ with $0 < x_A < 1$. In the applications to the deuteron ($A = D$) in Part II [1], this variable is denoted by $x_D$. The symbol $x$ (without subscript) is used for the rescaled variable $x \equiv 2x_D$, which takes values $0 < x < 2$ and can be interpreted as the scaling variable for scattering on the nucleon in the deuteron.

### B. Basis vectors

For describing the SIDIS process in a relativistically covariant manner it is useful to introduce a basis of orthonormal four-vectors derived from the particle momenta. One distinguishes the "longitudinal" subspace spanned by vectors $q$ and $P$ and the "transverse" subspace orthogonal to it.

In the longitudinal subspace we introduce two different sets of orthonormal vectors, adapted to different purposes as explained in the following. Set I consists of the vectors

$$e_q \equiv \frac{q}{\sqrt{-q^2}}, \quad e_L \equiv \frac{P + (e_q\cdot P)e_q}{\sqrt{P^2 + (e_q\cdot P)^2}}, \tag{2.6a}$$

$$e_q^2 = -1, \quad e_L^2 = 1, \quad e_q \cdot e_L = 0. \tag{2.6b}$$

Set II consists of the vectors

$$e_P \equiv \frac{P}{\sqrt{P^2}}, \quad e_{L*} \equiv \frac{q - (e_P\cdot q)e_P}{\sqrt{-q^2 + (e_P\cdot q)^2}}, \tag{2.7a}$$

$$e_P^2 = 1, \quad e_{L*}^2 = -1, \quad e_P \cdot e_{L*} = 0. \tag{2.7b}$$

The two sets are related by a hyperbolic rotation (equivalent to a Lorentz transformation),

$$e_L = \cosh\alpha\, e_P + \sinh\alpha\, e_{L*}, \tag{2.8a}$$

$$e_q = \sinh\alpha\, e_P + \cosh\alpha\, e_{L*}, \tag{2.8b}$$

$$\sinh\alpha = 1/\gamma, \quad \cosh\alpha = \sqrt{1+\gamma^2}/\gamma, \tag{2.8c}$$

where

$$\gamma \equiv \frac{\sqrt{-q^2P^2}}{q\cdot P} = \frac{2Mx_A}{Q}. \tag{2.9}$$

Both sets are complete in the longitudinal subspace,

$$e_L^\mu e_L^\nu - e_q^\mu e_q^\nu = e_P^\mu e_P^\nu - e_{L*}^\mu e_{L*}^\nu \equiv g_L^{\mu\nu}. \tag{2.10}$$

The projector on the transverse subspace is

$$g_T^{\mu\nu} \equiv g^{\mu\nu} - g_L^{\mu\nu}, \quad g^{\mu\nu} = g_L^{\mu\nu} + g_T^{\mu\nu}. \tag{2.11}$$

The transverse component of a four-vector $V^\mu$ is denoted as

$$V_T^\mu \equiv g_T^{\mu\nu} V_\nu, \quad V_T^2 < 0; \tag{2.12}$$

it is a spacelike four-vector, subject to the Lorentz metric. The antisymmetric tensor in the transverse subspace is

$$\epsilon_T^{\mu\nu} \equiv \epsilon^{\mu\nu\rho\sigma} e_{L,\rho} e_{q,\sigma} = \epsilon^{\mu\nu\rho\sigma} e_{P,\rho} e_{L*,\sigma}, \quad \epsilon^{0123} \equiv 1. \tag{2.13}$$

In the transverse subspace the basis vectors can be aligned either with the lepton momentum $l$ or with final hadron momentum $P_h$. We define basis vectors aligned with the lepton momentum as

$$e_x \equiv \frac{l_T}{\sqrt{-l_T^2}}, \quad e_y^\mu \equiv \epsilon_T^{\mu\nu} e_{x,\nu}, \quad e_x^2, e_y^2 = -1. \tag{2.14}$$

$e_x$ is along the lepton transverse momentum and $e_y$ is normal to it. Note that $e_x$ is a vector and $e_y$ is a pseudovector.

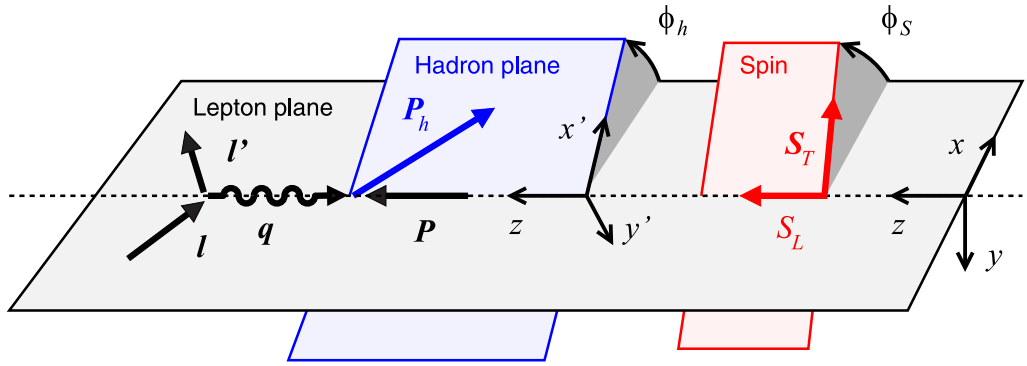



FIG. 1. Azimuthal angles and coordinate systems in the collinear frames. The angles $\phi_h$ and $\phi_S$ conform to the Trento convention [58]. The $xyz$ coordinate system is aligned with the lepton plane, with the $z$ direction opposite to $\boldsymbol{q}$ and the $x$ direction along $\boldsymbol{l}_T = \boldsymbol{l}'_T$. The $x'y'z$ coordinate system is aligned with the hadron plane, with the $x'$ direction along $\boldsymbol{P}_{hT}$.

In a similar way we define basis vectors aligned with the final hadron momentum as

$$e_{x'} \equiv \frac{P_{hT}}{\sqrt{-P_{hT}^2}}, \quad e_{y'}^{\mu} \equiv \epsilon_T^{\mu\nu} e_{x',\nu}, \quad e_{x',y'}^2 = -1. \tag{2.15}$$

The two sets of transverse four-vectors are related by a planar rotation

$$e_{x'} = \cos\phi_h e_x - \sin\phi_h e_y, \tag{2.16a}$$

$$e_{y'} = \sin\phi_h e_x + \cos\phi_h e_y. \tag{2.16b}$$

The angle $\phi_h$ can be expressed through the scalar products of the four-vectors,

$$\cos\phi_h = -e_x \cdot e_{x'}, \quad \sin\phi_h = e_y \cdot e_{x'}, \tag{2.17}$$

and is thus defined in a relativistically invariant manner and without reference to a coordinate system. The definition of the angle $\phi_h$ here follows the Trento convention [58] (see further discussion in Sec. II C). Note that the definition of the angle differs from the one in the earlier work of Ref. [39] (see Appendix A for reference). Both sets of basis vectors are complete in the transverse subspace

$$-e_x^{\mu} e_x^{\nu} - e_y^{\mu} e_y^{\nu} = -e_{x'}^{\mu} e_{x'}^{\nu} - e_{y'}^{\mu} e_{y'}^{\nu} = g_T^{\mu\nu}. \tag{2.18}$$

In summary, each of the four-vector sets

$$\{e_L, e_q, e_x, e_y\}, \quad \{e_P, e_{L*}, e_x, e_y\} \tag{2.19}$$

(or the equivalent sets with $e_{x'}, e_{y'}$) forms a natural basis of four-dimensional space-time and can be used to expand the vectors and tensors characterizing the scattering process; depending on the quantity, one or the other sets will be more convenient. The basis vectors are defined without reference to any specific frame or coordinate system and can be used accordingly. A simple geometric interpretation of the basis vectors becomes possible in the collinear frames described in the following subsection.

### C. Collinear frames

The SIDIS process is naturally described in a so-called collinear frame, defined by the condition that the momentum transfer and the target momentum be collinear three-vectors, $\boldsymbol{q} \parallel \boldsymbol{P}$ (see Fig. 1). The condition defines not a single frame but a class of frames whose members are related by boosts along the collinear axis. It contains several frames of special interest: the target rest frame ($\boldsymbol{P} = 0$), the virtual photon-target center-of-mass frame ($\boldsymbol{q} + \boldsymbol{P} = 0$), and a frame with zero energy transfer ($q^0 = 0$, Breit frame). The following discussion applies to any frame in the class and does not assume a specific member unless specified otherwise.

The collinear axis is chosen as the $z$ axis, with $\boldsymbol{q}$ pointing in the negative $z$ direction, $\boldsymbol{q} = q^z \boldsymbol{e}_z$ with $q^z < 0$. With this choice any frame reached by a boost along the $z$ axis will also have $q^z < 0$, because the sign of $q^z$ remains unchanged under boosts. This is because the four-vector $q$ is spacelike, $q^2 < 0$, and there is no frame where it can have $q^z = 0$, which would imply that only the time component is nonzero and the four-vector is timelike. The value of $q^z < 0$ serves as a boost parameter selecting a particular member of the class of collinear frames (other ways to select a frame based on light-front components are discussed in Part II [1]). The target momentum can have components $P^z > 0$ or $P^z < 0$, depending on the particular frame.

The components of the longitudinal basis four-vectors of Set I, Eq. (2.6), in the collinear frame can be expressed as

$$e_q = Q^{-1}(\omega, q^z \boldsymbol{e}_z), \quad e_L = Q^{-1}(-q^z, -\omega \boldsymbol{e}_z),$$
$$\omega \equiv \sqrt{(q^z)^2 - Q^2}, \quad |q^z| > Q, \quad q^z < 0. \tag{2.20}$$

The components of Set II can be obtained from Eq. (2.8).

The transverse component of the lepton momentum, together with the collinear axis, defines the lepton plane (see Fig. 1). We denote the coordinate system aligned with the lepton plane by $xyz$, with $x$ along the initial lepton transverse momentum (which is equal to the final transverse lepton momentum, because the momentum transfer is in the longitudinal direction), and $y$ along the normal direction, such that $xyz$ forms a right-handed system. In this coordinate system the basis four-vectors Eq. (2.14) have components

$$e_x = (0, \boldsymbol{e}_x), \quad e_y = (0, \boldsymbol{e}_y); \tag{2.21}$$

their spatial components coincide with the three-dimensional unit vectors along the directions. The transverse component of the final hadron momentum, together with the collinear

axis, defines the hadron plane (see Fig. 1). We denote the coordinate system aligned with the hadron plane by $x'y'z$, with $x'$ along the hadron transverse momentum and $y'$ the right-handed normal. The basis four-vectors Eq. (2.15) have components

$$e_{x'} = (0, \boldsymbol{e}_{x'}), \quad e_{y'} = (0, \boldsymbol{e}_{y'}). \tag{2.22}$$

Equations (2.21) and (2.22) describe the transverse basis vectors in any collinear frame; their form is not affected by boosts along the $z$ axis.

The angle $\phi_h$ in Eq. (2.16) becomes the angle between the lepton and the hadron planes in the collinear frame (see Fig. 1). It is defined according to the Trento convention [58] and takes values $\phi_h \in [0, 2\pi]$. In our coordinate systems $\phi_h$ is the angle of the rotation taking the $xy$ to the $x'y'$ axes, measured in the negative mathematical sense (rotation of the positive $x$ axis away from the positive $y$ axis). Hadron momenta with $P_h^y < 0$ ($>0$) have azimuthal angles $\phi_h < \pi$ ($> \pi$). Note that the angle is unambiguously defined in terms of the particle four-momenta by Eq. (2.17), which does not refer to a coordinate system. Reference [58] and other works use a coordinate system where the $z$ axis is along $\boldsymbol{q}$, which differs from ours by reversing the direction of the $z$ and $y$ axes (see Fig. 1); the expressions presented in the following could easily be transcribed to that coordinate system without changing the definition of $\phi_h$.

A special collinear frame is the target rest frame, where $P = (M, \boldsymbol{0})$. In this frame the longitudinal basis four-vectors of Set II Eq. (2.7) have components

$$e_P = (1, \boldsymbol{0}), \quad e_{L*} = (0, -\boldsymbol{e}_z). \tag{2.23}$$

The spatial component of $e_{L*}$ is the negative of the unit vector in the $z$ direction. When using the basis four-vectors of Set II (together with the transverse basis vectors) to expand vectors and tensors describing the scattering process, one can make a direct connection with the corresponding quantities in the target rest frame. In Sec. III we use the basis $\{e_P, e_{L*}, e_{x'}, e_{y'}\}$ to expand the target polarization vector and tensor and connect it with the rest-frame polarization.

It should be noted that in actual experiments the relation between the collinear frame and the laboratory frame depends on the final-state lepton and hadron momenta, which enter in the definition of the basis vectors. Even for fixed final lepton momentum (i.e., for fixed $x_A$ and $Q^2$) the orientation of the transverse vectors depends on the observed hadron momentum.

### D. Final-state hadron variables

The momentum of the final-state hadron in the SIDIS process is characterized by three kinematic variables. They refer to the hadron's longitudinal and transverse momentum in the collinear frame and can be defined in terms of invariants. The hadron transverse momentum is defined invariantly as the norm of the four-momentum projection on the transverse subspace, Eq. (2.12),

$$|\boldsymbol{P}_{hT}| \equiv \sqrt{-P_{hT}^2} = \sqrt{-(g_T \cdot P_h)^2}; \tag{2.24}$$

its angle $\phi_h$ is defined invariantly through the scalar products with the basis vectors aligned with the lepton momentum, Eq. (2.17). In the collinear frame, $|\boldsymbol{P}_{hT}|$ and $\phi_h$ describe the magnitude and azimuthal angle of the transverse momentum as specified in Fig. 1.

For the hadron longitudinal momentum several variables have been introduced, motivated by various physical considerations. One invariant variable is the ratio

$$z_h \equiv \frac{P_h \cdot P}{q \cdot P}, \quad 0 < z_h < 1, \tag{2.25}$$

which can be interpreted as the fraction of the virtual photon energy carried by the hadron in the target rest frame. This variable is commonly used in the analysis of SIDIS in the current fragmentation region, where $z_h = \mathcal{O}(1)$. Another variable is the hadron's longitudinal momentum $P_h^z$ in the virtual photon-target center-of-mass frame ($\boldsymbol{q} + \boldsymbol{P} = 0$, a special collinear frame), expressed in terms of the Feynman scaling variable

$$x_F \equiv -P_h^z / P_{h,\max}^z, \quad -1 < x_F < 1, \tag{2.26}$$

where $P_{h,\max}^z$ is the maximum longitudinal momentum for the given center-of-mass energy and hadron mass; the minus sign in Eq. (2.26) is the result of our convention $q^z < 0$ [38]. In this variable the current fragmentation region is identified as $x_F \approx 1$, the target fragmentation region as $x_F \approx -1$.

Particularly useful variables can be constructed from the light-front momentum components of the final-state hadron in the collinear frames. They are defined as $P_h^\pm \equiv P_h^0 \pm P_h^z$, with

$$P_h^+ P_h^- - |\boldsymbol{P}_{hT}|^2 = P_h^2 = M_h^2, \tag{2.27}$$

and have values $P_h^+ > 0$ and $P_h^- > 0$. The target and virtual photon four-momenta in the collinear frames have light-front components [38,39]

$$P^+ > 0 \text{ (arbitrary)}, \quad P^- = M^2/P^+ > 0, \tag{2.28a}$$

$$q^+ = -\xi_A P^+ < 0, \quad q^- = Q^2 \xi_A / P^+ > 0, \tag{2.28b}$$

where

$$\xi_A \equiv \frac{2x_A}{1 + \sqrt{1 + \gamma^2}}; \tag{2.29}$$

the value of $P^+$ is arbitrary and serves as a boost parameter. The four-momentum of the total hadronic final state, $q + P$, has light-front components

$$(q+P)^+ = (1 - \xi_A) P^+ > 0, \tag{2.30a}$$

$$(q+P)^- = (M^2 + Q^2/\xi_A)/P^+ > 0, \tag{2.30b}$$

and their product is equal to the invariant mass of the total hadronic final state (or the squared virtual photon-hadron center-of-mass energy),

$$W^2 \equiv (q+P)^2 = (q+P)^+ (q+P)^- = \left(M^2 + \frac{Q^2}{\xi_A}\right)(1 - \xi_A) = M^2 + \frac{1 - x_A}{x_A} Q^2. \tag{2.31}$$

The light-front momentum components of the identified hadron can then be expressed as fractions of the components

of the total hadronic final state,

$$P_h^+ = \zeta_h (q+P)^+, \quad 0 < \zeta_h < 1, \tag{2.32a}$$

$$P_h^- = \eta_h (q+P)^-, \quad 0 < \eta_h < 1. \tag{2.32b}$$

The fractions $\zeta_h$ and $\eta_h$ are boost invariant and have the same value in any collinear frame. The two variables are connected through the hadron mass shell condition [see Eqs. (2.27) and (2.31)],

$$\zeta_h \eta_h = \frac{M_h^2 + |\boldsymbol{P}_{hT}|^2}{W^2} \equiv \frac{M_{hT}^2}{W^2}, \tag{2.33}$$

and one can use one or the other to characterize the hadron longitudinal momentum.[2] In the DIS limit $W^2 \sim Q^2 \gg M_{hT}^2$, in the current fragmentation region $\eta_h = \mathcal{O}(1)$ and $\zeta_h = \mathcal{O}(M_{hT}^2/W^2)$, and

$$z_h = \eta_h \big[1 + \mathcal{O}\big(M_{hT}^2/W^2, M^2/W^2\big)\big]. \tag{2.34}$$

In the target fragmentation region $\zeta_h = \mathcal{O}(1)$ and $\eta_h = \mathcal{O}(M_{hT}^2/W^2)$, and

$$x_F = -\zeta_h \big[1 + \mathcal{O}\big(M_{hT}^2/W^2, M^2/W^2\big)\big]. \tag{2.35}$$

The light-front momentum fractions thus match with the conventional energy/momentum fraction variables in the DIS limit. The light-front momentum fractions have the advantage that they have simple properties also away from the DIS limit (kinematic limits, behavior in current and target fragmentation regions, integration measure); as such they are the preferred variables for describing semi-inclusive hadron production at finite energies.

The light-front momentum fractions can be expressed as scalar products with the basis four-vectors,

$$\zeta_h = \frac{P_h^+}{(q+P)^+} = \frac{(e_P + e_{L*}) \cdot P_h}{(e_P + e_{L*}) \cdot (q+P)}, \tag{2.36a}$$

$$\eta_h = \frac{P_h^-}{(q+P)^-} = \frac{(e_P - e_{L*}) \cdot P_h}{(e_P - e_{L*}) \cdot (q+P)}. \tag{2.36b}$$

This can be shown by evaluating the expressions in the target rest frame, where the basis vector components are given by Eq. (2.23), and using fact that the fractions are invariant under boosts. Equations (2.36) can be used to compute the fractions from the particle four-momenta given in any frame, without knowing their coordinates in the collinear frame.

The variables $\zeta_h$ and $\eta_h$ measure the hadron light-front momentum components $P_h^\pm$ as fractions of the components of the total hadronic final state, $(q+P)^\pm$. Alternatively, one can measure them as fractions of the components of the target momentum, $P^\pm$; the two definitions are related by a simple factor. In Part II [1] we use a rescaled version of the light-front momentum fraction $P_h^+/P^+$ in describing nuclear breakup as a special case of target fragmentation.

The invariant phase-space element in the identified hadron momentum is defined as

$$d\Gamma_{P_h} \equiv \frac{d^4 P_h}{(2\pi)^4}\, 2\pi\delta\big(P_h^2 - M_h^2\big)\theta\big(P_h^0\big). \tag{2.37}$$

In terms of the hadron three-momentum in any frame, it takes the form

$$d\Gamma_{P_h} = \frac{d^3 P_h}{2(2\pi)^3 E_h(\boldsymbol{P}_h)}. \tag{2.38}$$

In terms of the hadron light-front momentum components in the collinear frames, the phase-space element can be expressed as

$$d\Gamma_{P_h} = \frac{dP_h^+ d^2 P_{hT}}{2(2\pi)^3 P_h^+} = \frac{1}{2(2\pi)^3}\frac{d\zeta_h}{\zeta_h} d^2 P_{hT}, \tag{2.39}$$

or alternatively as

$$d\Gamma_{P_h} = \frac{dP_h^- d^2 P_{hT}}{2(2\pi)^3 P_h^-} = \frac{1}{2(2\pi)^3}\frac{d\eta_h}{\eta_h} d^2 P_{hT}; \tag{2.40}$$

the two forms are equivalent, and each one can be used in the entire phase space with appropriate kinematic limits (including current and target fragmentation regions). The light-front variables result in a simple form of the phase-space element. The integration measure factorizes the longitudinal and transverse momenta and enables separation of the two variables. In contrast, in the representation in three-momentum variables, Eq. (2.38), the factor $1/E_h$ depends on both longitudinal and transverse momenta, and separation only becomes possible in limit $P_h^z \gg M_{hT}$. The kinematic limits of the light-front momentum variables can be easily determined by solving the conditions of energy and momentum conservation in the light-front momentum variables, for finite $W$ and a finite hadron mass $M_h$.

## III. POLARIZED SPIN-1 TARGET

### A. Covariant spin-1 density matrix

The mixed spin state of the spin-1 target in the scattering process Eq. (2.1) is described by a density matrix. We now determine the general form of this matrix for a moving target, its parametrization through invariant polarization parameters, and the expansion of the density matrix in the basis four-vectors of Sec. II.

Pure spin states of a spin-1 particle with mass $M$ and four-momentum $P$ are described covariantly by a four-vector wave function $\epsilon^\alpha(\lambda)$, with

$$P^\alpha \epsilon_\alpha(\lambda) = 0, \tag{3.1a}$$

$$\epsilon^{\alpha *}(\lambda)\epsilon_\alpha(\lambda') = -\delta(\lambda, \lambda'), \tag{3.1b}$$

$$\sum_\lambda \epsilon^\alpha(\lambda)\epsilon^{\beta *}(\lambda) = -g^{\alpha\beta} + \frac{P^\alpha P^\beta}{M^2}. \tag{3.1c}$$

$\lambda = (+1, 0, -1)$ denotes the spin quantum number. Here and in the following, it is assumed that the wave function of the

[2]Here we use the light-front components to describe the four-momentum of the physical hadron $h$, where plus and minus components are both on-shell and related by Eq. (2.27), and either can be used as independent variable. In Part II [1] we use light-front quantization, where the plus component acts as "momentum" and the minus component as "energy," and the energy can be off-shell in intermediate states of the reaction; this distinction is not relevant here.

moving particle is obtained from that of the particle at rest by a boost,

$$\epsilon^\alpha(\lambda|\boldsymbol{P}=0) \to \epsilon^\alpha(\lambda|\boldsymbol{P}), \tag{3.2}$$

and $\lambda$ is understood as the spin projection in the particle's rest frame with respect to a given axis. The specific form of the moving wave function depends on the choice of the boost; e.g., canonical boosts (along the direction of $\boldsymbol{P}$) or light-front boosts (a sequence of boosts along the longitudinal and transverse directions). The following considerations apply to any choice of the boost.

A mixed spin state of the spin-1 particle in the rest frame is described by a density matrix $\rho(\lambda,\lambda')$, a Hermitean $3\times 3$ matrix with unit trace,

$$\rho(\lambda,\lambda') = \rho^*(\lambda',\lambda), \tag{3.3a}$$

$$\sum_\lambda \rho(\lambda,\lambda) = 1. \tag{3.3b}$$

In analogy with the description of pure states, the mixed state of the moving particle is then described covariantly by a four-tensor density matrix

$$\rho^{\alpha\beta} \equiv \sum_{\lambda,\lambda'} \rho(\lambda,\lambda')\epsilon^\alpha(\lambda)\epsilon^{*\beta}(\lambda'), \tag{3.4}$$

with

$$P_\alpha \rho^{\alpha\beta} = 0, \quad \rho^{\alpha\beta}P_\beta = 0, \tag{3.5a}$$

$$\rho^{\alpha\beta} = \rho^{\beta\alpha *}, \tag{3.5b}$$

$$\rho^\alpha{}_\alpha = -1. \tag{3.5c}$$

A spin observable characterizing the spin-1 system is given by a matrix in the spin quantum numbers, $O(\lambda',\lambda)$, which may be of four-vector or tensor character and carry additional indices not shown here. In the four-tensor representation it corresponds to a bilinear form

$$O(\lambda',\lambda) \equiv \epsilon^{\beta *}(\lambda')O_{\beta\alpha}\epsilon^\alpha(\lambda), \tag{3.6}$$

where $O_{\beta\alpha}$ is a tensor in the indices $\alpha,\beta$. The expectation value in the mixed state is computed as

$$\langle O\rangle \equiv \sum_{\lambda,\lambda'} \rho(\lambda,\lambda')O(\lambda',\lambda) = \rho^{\alpha\beta}O_{\beta\alpha}. \tag{3.7}$$

As a special case, the three-dimensional matrix elements $\rho(\lambda,\lambda')$ are obtained by choosing $O_{\beta\alpha}$ as the tensor product of the corresponding four-vectors,

$$\rho(\lambda,\lambda') = \rho^{\alpha\beta}\epsilon_\beta(\lambda')\epsilon^*_\alpha(\lambda). \tag{3.8}$$

This formula can be used to evaluate the elements of the rest-frame density matrix in any frame where the particle is moving if the explicit form of the four-vector wave functions is known.

The four-tensor density matrix Eq. (3.4) can be parametrized covariantly as

$$\rho^{\alpha\beta} = \frac{1}{3}\left(-g^{\alpha\beta} + \frac{P^\alpha P^\beta}{M^2}\right) + \frac{i}{2M}\epsilon^{\alpha\beta\gamma\delta}P_\gamma S_\delta - T^{\alpha\beta}. \tag{3.9}$$

The terms are known as the unpolarized, vector-polarized, and tensor-polarized term. The parameters are the real axial four-vector $S^\alpha$,

$$P^\alpha S_\alpha = 0, \tag{3.10}$$

and the real symmetric traceless four-tensor $T^{\alpha\beta}$,

$$P_\alpha T^{\alpha\beta} = 0, \quad T^{\alpha\beta}P_\beta = 0, \tag{3.11a}$$

$$T^{\alpha\beta} = T^{\beta\alpha}, \tag{3.11b}$$

$$T^\alpha{}_\alpha = 0. \tag{3.11c}$$

The form of Eq. (3.9) follows from the conditions of Eq. (3.5). It applies to any choice of boost defining the moving spin states, Eq. (3.2); the differences between choices are encoded in the values of the parameters $S^\alpha$ and $T^{\alpha\beta}$. Thus the polarization of the moving spin-1 particle is completely specified by the covariant parameters $S^\alpha$ and $T^{\alpha\beta}$ and can be evaluated in any frame.

### B. Invariant polarization parameters

For describing the scattering process Eq. (2.1) we expand the parameters of Eq. (3.9) in the basis four-vectors of Sec. II. Since $S^\alpha$ and $T^{\alpha\beta}$ are orthogonal to the target four-momentum $P^\mu$, it is convenient to expand them in the longitudinal vectors of Set II, Eq. (2.7). For the transverse vectors we use the ones aligned with the final-state hadron momentum, Eq. (2.15). We define the expansion coefficients as

$$e_{L*}\cdot S \equiv S_L, \tag{3.12a}$$

$$-e_{x'}\cdot S \equiv S_T\cos(\phi_S-\phi_h), \tag{3.12b}$$

$$-e_{y'}\cdot S \equiv -S_T\sin(\phi_S-\phi_h), \tag{3.12c}$$

$$e_{L*}\cdot T\cdot e_{L*} \equiv T_{LL}, \tag{3.12d}$$

$$-e_{L*}\cdot T\cdot e_{x'} \equiv T_{LT}\cos(\phi_{T_L}-\phi_h), \tag{3.12e}$$

$$-e_{L*}\cdot T\cdot e_{y'} \equiv -T_{LT}\sin(\phi_{T_L}-\phi_h), \tag{3.12f}$$

$$e_{x'}\cdot T\cdot e_{x'} - e_{y'}\cdot T\cdot e_{y'} \equiv T_{TT}\cos(2\phi_{T_T}-2\phi_h), \tag{3.12g}$$

$$e_{x'}\cdot T\cdot e_{y'} \equiv -\tfrac{1}{2}T_{TT}\sin(2\phi_{T_T}-2\phi_h). \tag{3.12h}$$

The vector polarization is now expressed by the three parameters $\{S_L, S_T, \phi_S\}$, and the tensor polarization by the five parameters $\{T_{LL}, T_{LT}, T_{TT}, \phi_{T_L}, \phi_{T_T}\}$. Notice that we do not introduce an additional parameter for $e_{x'}\cdot T\cdot e_{x'} + e_{y'}\cdot T\cdot e_{y'}$, as this combination is equal to $-e_{L*}\cdot T\cdot e_{L*}$) due to the zero trace of the tensor $T$ [Eq. (3.11)]. The parameters are defined in terms of scalar products of four-vectors and are thus invariant. We refer to them as the invariant polarization parameters. The parameters $S_T$, $T_{LT}$, and $T_{TT}$ are $\geqslant 0$ and can be interpreted as intensities; this can be shown by evaluating the invariant parameters in the target rest frame.

In Eq. (3.12) the polarization four-vector and tensor are contracted with the basis vector $e_{L*}$ of Set II. Because of the conditions Eq. (3.10) and (3.11), these contractions can equivalently be computed with the basis vector $e_q$ of Set I,

related to $e_{L*}$ by Eq. (2.8),

$$S_L = e_{L*} \cdot S = \frac{\gamma}{\sqrt{1+\gamma^2}}\, e_q \cdot S, \tag{3.13}$$

and similarly for the contractions with $T$. These relations will be used when evaluating the polarized cross section in Sec. IV B.

The invariant polarization parameters include scalars with even and odd parity. The parity can be inferred from the parity of the vectors and tensors entering in the scalar products. One finds

$$\text{even:}\quad e_{y'} \cdot S,\ e_{L*} \cdot T \cdot e_{L*},\ e_{L*} \cdot T \cdot e_{x'},\ e_{x'} \cdot T \cdot e_{x'} - e_{y'} \cdot T \cdot e_{y'}, \tag{3.14a}$$

$$\text{odd:}\quad e_{L*} \cdot S,\ e_{x'} \cdot S,\ e_{L*} \cdot T \cdot e_{y'},\ e_{x'} \cdot T \cdot e_{y'}. \tag{3.14b}$$

These properties will be used in the decomposition of the polarized cross section in Sec. IV B.

The invariant polarization parameters have a simple interpretation in the class of collinear frames, which contains the target rest frame as a special case (see Sec. II). In the target rest frame, the polarization four-vector and four-tensor have only spatial components

$$S^0 = 0, \quad S^i \neq 0, \tag{3.15a}$$

$$T^{0\beta}, T^{\alpha 0} = 0, \quad T^{ij} \neq 0, \tag{3.15b}$$

and the basis four-vectors are given by Eqs. (2.22) and (2.23). The contractions in Eq. (3.12) become

$$e_{L*} \cdot S = \boldsymbol{e}_z \cdot \boldsymbol{S} = S^z, \tag{3.16a}$$

$$-e_{x'} \cdot S = \boldsymbol{e}_{x'} \cdot \boldsymbol{S} = S^{x'}, \tag{3.16b}$$

$$-e_{y'} \cdot S = \boldsymbol{e}_{y'} \cdot \boldsymbol{S} = S^{y'}, \tag{3.16c}$$

$$e_{L*} \cdot T \cdot e_{L*} = \boldsymbol{e}_z \cdot T \cdot \boldsymbol{e}_z = T^{zz}, \quad \text{etc.} \tag{3.16d}$$

This directly connects the invariant polarization parameters with the target spin state in the rest frame and can be used for polarization preparation (see Sec. V A) and dynamical calculations (see Part II [1]). Note that $S_L = +1$ corresponds to spin projection $S^z = +1$ on the $z$ axis, opposite to the direction of $\boldsymbol{q}$, in agreement with the convention used for the spin-1/2 target [58]. The angle $\phi_S$ is the azimuthal angle of the transverse vector polarization, and $\phi_{T_L}$ and $\phi_{T_T}$ are the azimuthal angles characterizing the transverse directions of the tensor polarization; their definition conforms to the Trento convention [58].

In the argument of the trigonometric functions in Eq. (3.12) the polarization angles $\phi_S, \phi_{T_L}, \phi_{T_T}$ appear before the hadron angle $\phi_h$, as is natural when projecting the polarization vector/tensor on the basis vectors aligned with the hadron plane. In the following we write the arguments such that $\phi_h$ comes before the polarization angles, which is standard in the presentation of the SIDIS cross section (see Sec. IV),

$$\cos(\phi_S - \phi_h) \to \cos(\phi_h - \phi_S), \tag{3.17a}$$

$$\sin(\phi_S - \phi_h) \to -\sin(\phi_h - \phi_S), \quad \text{etc.} \tag{3.17b}$$

This results in the appearance of a minus sign in the structures proportional to sine functions, which cancels the minus sign already present in Eq. (3.12).

### C. Tensor representation

The four-tensor density matrix can be expanded in tensors formed from the basis vectors Eqs. (2.7) and (2.15), with the coefficients given by the invariant polarization parameters. This representation is useful because it expresses the four-dimensional density matrix explicitly in terms of the invariant polarization parameters. It can also be connected with the three-dimensional Cartesian components of the density matrix in the rest frame and its angular momentum decomposition.

The four-vector parameter $S$ in Eq. (3.9) is expanded in the orthonormal basis vectors as

$$S^\alpha = -S_L e^\alpha_{L*} + S_T\big[\cos(\phi_h - \phi_S) e^\alpha_{x'} + \sin(\phi_h - \phi_S) e^\alpha_{y'}\big]. \tag{3.18}$$

To expand the four-tensor parameter $T$, we form the basis tensors

$$e^{\alpha\beta}_{LL} = \frac{1}{\sqrt{6}}\big(2e^\alpha_{L*}e^\beta_{L*} - e^\alpha_{x'}e^\beta_{x'} - e^\alpha_{y'}e^\beta_{y'}\big), \tag{3.19a}$$

$$e^{\alpha\beta}_{LT} = \frac{1}{\sqrt{2}}\big(-e^\alpha_{L*}e^\beta_{x'} - e^\alpha_{x'}e^\beta_{L*}\big), \tag{3.19b}$$

$$e^{\alpha\beta}_{LT'} = \frac{1}{\sqrt{2}}\big(-e^\alpha_{L*}e^\beta_{y'} - e^\alpha_{y'}e^\beta_{L*}\big), \tag{3.19c}$$

$$e^{\alpha\beta}_{TT} = \frac{1}{\sqrt{2}}\big(e^\alpha_{x'}e^\beta_{x'} - e^\alpha_{y'}e^\beta_{y'}\big), \tag{3.19d}$$

$$e^{\alpha\beta}_{TT'} = \frac{1}{\sqrt{2}}\big(e^\alpha_{x'}e^\beta_{y'} + e^\alpha_{y'}e^\beta_{x'}\big), \tag{3.19e}$$

which are real, traceless, and normalized such that

$$e^{\alpha\beta}_I e^{\alpha\beta}_{I'} = \delta_{II'} \quad (I = LL, LT, LT', TT, TT'). \tag{3.20}$$

The tensor $T$ is expanded in these basis tensors as

$$\begin{aligned} T^{\alpha\beta} = &\sqrt{\frac{3}{2}}\, T_{LL} e^{\alpha\beta}_{LL} + \sqrt{2}\, T_{LT} \cos(\phi_h - \phi_{T_L}) e^{\alpha\beta}_{LT} \\ &+ \sqrt{2}\, T_{LT} \sin(\phi_h - \phi_{T_L}) e^{\alpha\beta}_{LT'} \\ &+ \frac{1}{\sqrt{2}}\, T_{TT} \cos(2\phi_h - 2\phi_{T_T}) e^{\alpha\beta}_{TT} \\ &+ \frac{1}{\sqrt{2}}\, T_{TT} \sin(2\phi_h - 2\phi_{T_T}) e^{\alpha\beta}_{TT'}. \end{aligned} \tag{3.21}$$

The expansion coefficients can be determined by contracting both sides of Eq. (3.21) with the basis tensors, using the orthogonality condition Eq. (3.20) and the expressions of the contractions in Eq. (3.12).

In the target rest frame the polarization four-vector and four-tensor have only spatial components, Eq. (3.15), and the basis four-vectors are given by Eqs. (2.22) and (2.23). The expansion of the polarization vector, Eq. (3.18), becomes

$$\boldsymbol{S} = S_L \boldsymbol{e}_z + S_T[\cos(\phi_h - \phi_S)\boldsymbol{e}_{x'} + \sin(\phi_h - \phi_S)\boldsymbol{e}_{y'}]. \tag{3.22}$$

The expansion of the polarization tensor becomes (here $i, j = 1,2,3$)

$$\begin{aligned} T^{ij} =& \sqrt{\frac{3}{2}}\, T_{LL} e^{ij}_{LL} + \sqrt{2}\, T_{LT} \cos(\phi_h - \phi_{T_L}) e^{ij}_{LT} \\ &+ \sqrt{2}\, T_{LT} \sin(\phi_h - \phi_{T_L}) e^{ij}_{LT'} \\ &+ \frac{1}{\sqrt{2}}\, T_{TT} \cos(2\phi_h - 2\phi_{T_T}) e^{ij}_{TT} \\ &+ \frac{1}{\sqrt{2}}\, T_{TT} \sin(2\phi_h - 2\phi_{T_T}) e^{ij}_{TT'}, \end{aligned} \tag{3.23}$$

where the spatial components of the basis tensors are given by

$$e^{ij}_{LL} = \frac{1}{\sqrt{6}}\left(3e^i_z e^j_z - \delta^{ij}\right) = \mathcal{Y}^{ij}_{20} \tag{3.24a}$$

$$\begin{aligned} e^{ij}_{LT} &= \frac{1}{\sqrt{2}}\left(e^i_z e^j_{x'} + e^i_{x'} e^j_z\right) \\ &= -\frac{1}{\sqrt{2}}\left(\mathcal{Y}^{ij}_{21} - \mathcal{Y}^{ij}_{2-1}\right), \end{aligned} \tag{3.24b}$$

$$\begin{aligned} e^{ij}_{LT'} &= \frac{1}{\sqrt{2}}\left(e^i_z e^j_{y'} + e^i_{y'} e^j_z\right) \\ &= \frac{i}{\sqrt{2}}\left(\mathcal{Y}^{ij}_{21} + \mathcal{Y}^{ij}_{2-1}\right), \end{aligned} \tag{3.24c}$$

$$\begin{aligned} e^{ij}_{TT} &= \frac{1}{\sqrt{2}}\left(e^i_{x'} e^j_{x'} - e^i_{y'} e^j_{y'}\right), \\ &= \frac{1}{\sqrt{2}}\left(\mathcal{Y}^{ij}_{22} + \mathcal{Y}^{ij}_{2-2}\right), \end{aligned} \tag{3.24d}$$

$$\begin{aligned} e^{ij}_{TT'} &= \frac{1}{\sqrt{2}}\left(e^i_{x'} e^j_{y'} + e^i_{y'} e^j_{x'}\right) \\ &= -\frac{i}{\sqrt{2}}\left(\mathcal{Y}^{ij}_{22} - \mathcal{Y}^{ij}_{2-2}\right). \end{aligned} \tag{3.24e}$$

Here $\mathcal{Y}_{LM}$ are the three-dimensional spherical tensors with angular momentum $L = 2$ and projection $M = 0, \pm 1, \pm 2$ on the $z$ axis (see, e.g., Ref. [59])

$$\mathcal{Y}_{20} = \frac{1}{\sqrt{6}}(3\boldsymbol{e}_z \otimes \boldsymbol{e}_z - 1), \tag{3.25a}$$

$$\mathcal{Y}_{2\pm1} = \mp\frac{1}{\sqrt{2}}(\boldsymbol{e}_z \otimes \boldsymbol{e}_\pm + \boldsymbol{e}_\pm \otimes \boldsymbol{e}_z), \tag{3.25b}$$

$$\mathcal{Y}_{2\pm2} = \boldsymbol{e}_\pm \otimes \boldsymbol{e}_\pm \qquad \left[\boldsymbol{e}_\pm \equiv \frac{1}{\sqrt{2}}(\boldsymbol{e}_{x'} \pm i\boldsymbol{e}_{y'})\right], \tag{3.25c}$$

whose projections on a unit vector $\boldsymbol{n}$ are the spherical harmonics with $L = 2$

$$\boldsymbol{n} \cdot \mathcal{Y}_{2M} \cdot \boldsymbol{n} = \sqrt{\frac{2 \cdot 4\pi}{5 \cdot 3}}\, Y_{2M}(\boldsymbol{n}). \tag{3.26}$$

The four-dimensional expansion Eq. (3.21) thus follows the angular momentum decomposition of the three-dimensional polarization tensor in the target rest frame and connects it with the invariant polarization parameters. In dynamical calculations Eq. (3.21) can be used to compute the cross section proportional to a given invariant polarization parameter (see Part II [1]).

### D. Spin quantum number representation

From the basis vectors $e_{L*}$ and $e_{x'}, e_{y'}$ one can also construct a set of four-vector spin wave functions $\epsilon(\lambda)$ for the spin-1 particle,

$$\epsilon^\alpha(\lambda = 0) = -e^\alpha_{L*}, \tag{3.27a}$$

$$\epsilon^\alpha(\lambda = \pm 1) = \mp\frac{1}{\sqrt{2}}\left(e^\alpha_{x'} \pm i e^\alpha_{y'}\right). \tag{3.27b}$$

In the collinear frame these vectors are aligned with the $z$ and $x', y'$ directions, and the polarization states correspond to spin projection 0 and $\pm 1$ on the $z$ axis (see Fig. 1). These vectors can be regarded as the result of a boost of the corresponding rest frame vectors, as indicated in Eq. (3.2). (For collinear boosts (along the $z$ axis) canonical and light-front boosts coincide, so there is no ambiguity in the definition of the spin wave function of a target with zero transverse momentum; this fact will be used in the dynamical calculations using light-front quantization in Part II [1].) Using Eq. (3.8) and the spin wave functions Eq. (3.27), we can now compute the density matrix in the spin quantum number representation. We obtain

$$\rho(\lambda, \lambda') = \begin{bmatrix} \frac{1}{3} + \frac{1}{2}S_L + \frac{1}{2}T_{LL} & \frac{1}{2\sqrt{2}}S_T e^{-i(\phi_h - \phi_S)} + \frac{1}{\sqrt{2}}T_{LT} e^{-i(\phi_h - \phi_{T_L})} & \frac{1}{2}T_{TT} e^{-i(2\phi_h - 2\phi_{T_T})} \\ \frac{1}{2\sqrt{2}}S_T e^{i(\phi_h - \phi_S)} + \frac{1}{\sqrt{2}}T_{LT} e^{i(\phi_h - \phi_{T_L})} & \frac{1}{3} - T_{LL} & \frac{1}{2\sqrt{2}}S_T e^{-i(\phi_h - \phi_S)} - \frac{1}{\sqrt{2}}T_{LT} e^{-i(\phi_h - \phi_{T_L})} \\ \frac{1}{2}T_{TT} e^{i(2\phi_h - 2\phi_{T_T})} & \frac{1}{2\sqrt{2}}S_T e^{i(\phi_h - \phi_S)} - \frac{1}{\sqrt{2}}T_{LT} e^{i(\phi_h - \phi_{T_L})} & \frac{1}{3} - \frac{1}{2}S_L + \frac{1}{2}T_{LL} \end{bmatrix}. \tag{3.28}$$

Equation (3.28) expresses the three-dimensional density matrix in the spin quantum numbers in terms of the intensity and angle parameters characterizing the vector and tensor polarization. It can be used to evaluate spin

observables in the spin quantum number representation Eq. (3.7).

In the treatment here we have introduced the density matrix in the four-dimensional representation, specified its form using its four-dimensional properties, and then derived the three-dimensional representation. In Appendix B we present an alternative approach, where we start with the specific form of the three-dimensional density matrix and derive its four-dimensional extension. That formulation is useful for connecting with the treatment of spin-1 systems in nonrelativistic physics.

## IV. CROSS SECTION

### A. Semi-inclusive hadronic tensor

The differential cross section for SIDIS on a spin-1 target can be computed using standard methods [60]. The hadronic structure is abstracted in the hadronic tensor of the process, whose structural decomposition can be determined from general considerations. We now perform the decomposition of the hadronic tensor and derive the form of the semi-inclusive cross section for the spin-1 target.

The differential cross section for semi-inclusive scattering Eq. (2.1), on a spin-1 target characterized by a spin density matrix $\rho$, is given by

$$\begin{aligned} d\sigma = &\frac{1}{4I}\sum_{\lambda_{e'}\lambda_h}\sum_{\lambda'\lambda}\rho(\lambda,\lambda') \\ &\times\sum_X \mathcal{M}(\lambda_{e'},\lambda_h;\lambda_e,\lambda')^*\mathcal{M}(\lambda_{e'},\lambda_h;\lambda_e,\lambda) \\ &\times(2\pi)^4\delta^{(4)}(P+q-P_h-P_X)\,d\Gamma_{l'}\,d\Gamma_{P_h}. \end{aligned} \tag{4.1}$$

Here

$$I \equiv \sqrt{(P\cdot l)^2} = \tfrac{1}{2}(s-M^2) \tag{4.2}$$

is the invariant flux factor (we neglect the lepton mass). $\mathcal{M}$ is the scattering amplitude of the process $e+A\to e'+X+h$, where $h$ is the identified hadron and $X$ is a multihadron remnant state; the amplitude is normalized according to the relativistic convention [60]. In Eq. (4.1) we indicate only the dependence of the amplitude on the spin variables: the initial and final lepton helicities, $\lambda_e$ and $\lambda_{e'}$; the target spin projection $\lambda$; and the identified hadron spin, $\lambda_h$. We do not indicate the dependence on the particle momenta or any of the variables of the multihadron state. The spin variables of the final state, $\lambda_{e'}$ and $\lambda_h$, are summed over. The target spin projections in the initial state, $\lambda$ and $\lambda'$ in the amplitude and its complex conjugate, are averaged over with the density matrix $\rho(\lambda,\lambda')$. $d\Gamma_{l'}$ is the invariant phase-space element of the final lepton

$$d\Gamma_{l'} \equiv \frac{d^4l'}{(2\pi)^4}\,2\pi\delta(l'^2)\theta(l'^0) = \frac{d^3l'}{2|\boldsymbol{l}'|(2\pi)^3}; \tag{4.3}$$

$d\Gamma_h$ is the one for the final hadron given in Eq. (2.37). The summation over $X$ in Eq. (4.1) denotes both the integration over the variables of the individual multihadron remnant state $X$ and the summation over all the allowed states. The $\delta$ function ensures four-momentum (energy and momentum) conservation.[3]

In leading order of the electromagnetic coupling (one-photon exchange approximation) the scattering amplitude is given by the product of the electromagnetic currents of the lepton and hadron transitions,

$$\begin{aligned} &\mathcal{M}(\lambda_{e'},\lambda_h;\lambda_e,\lambda) \\ &\quad= -\frac{e^2}{Q^2}\,\langle e'(\lambda_{e'})|J_\mu|e(\lambda_e)\rangle\;\langle X,h(\lambda_h)|J^\mu|A(\lambda)\rangle, \end{aligned} \tag{4.4}$$

where $e$ is the elementary charge. The cross section can then be expressed in terms of a leptonic and hadronic scattering tensor in the standard fashion. The leptonic tensor is defined as

$$L^{\mu\nu} \equiv \sum_{\lambda_{e'}}\langle e(\lambda_e)|J^{\dagger\mu}|e'(\lambda_{e'})\rangle\langle e'(\lambda_{e'})|J^\nu|e(\lambda_e)\rangle \tag{4.5a}$$

$$= 4l^\mu l^\nu - Q^2 g^{\mu\nu} - 2l^{\{\mu}q^{\nu\}} + (2\lambda_e)2i\epsilon^{\mu\nu\rho\sigma}q_\rho l_\sigma, \tag{4.5b}$$

where $\lambda_{e'}=\lambda_e$ in the sum (the lepton helicity is conserved by the interaction because we neglect the lepton mass). Here and in the following we use $\{...\}$ and $[...]$ to denote symmetrization and antisymmetrization in Lorentz indices,

$$a^{\{\mu}b^{\nu\}} = a^\mu b^\nu + b^\nu a^\mu, \quad a^{[\mu}b^{\nu]} = a^\mu b^\nu - b^\nu a^\mu. \tag{4.6}$$

One refers to the symmetric, lepton helicity-independent and antisymmetric, lepton-helicity-dependent parts as the unpolarized and polarized parts of the leptonic tensor. The hadronic tensor is defined as

$$\begin{aligned} W^{\mu\nu}(\lambda',\lambda) \equiv &\frac{1}{4\pi}\sum_{\lambda_h}\sum_X (2\pi)^4\delta^4(P+q-P_h-P_X) \\ &\times\langle A(\lambda')|J^{\dagger\mu}|X,h(\lambda_h)\rangle\langle X,h(\lambda_h)|J^\nu|A(\lambda)\rangle. \end{aligned} \tag{4.7}$$

Notice that the tensor is a matrix in the spin quantum numbers of the target states in the current matrix element and its complex conjugate ($\lambda'\neq\lambda$). It is assumed that the target spin states are prepared in the same way as those in the density

[3] In the simplified derivation here we assume that the scattering events contributing to the semi-inclusive cross section have exactly one hadron $h$ in the phase-space element at the given momentum $P_h$ and that the hadrons in the remnant state $X$ are kinematically distinct from the identified hadron. This allows us to express the cross section in terms of the scattering amplitudes without accounting for the hadron multiplicity. The results for the cross-section decomposition are not affected by this simplification; the representation in terms of amplitudes is used only to explain the origin of the hadronic tensor. The amplitude-level representation of the cross section can be generalized to account for final states with multiple hadrons $h$; see, e.g., Ref. [61].

matrix (see Sec. III). With these definitions one has

$$\sum_{\lambda_{e'}\lambda_h}\sum_{\lambda'\lambda}\rho(\lambda,\lambda')\sum_X \mathcal{M}(\lambda_{e'},\lambda_h;\lambda_e,\lambda')^*\mathcal{M}(\lambda_{e'},\lambda_h;\lambda_e,\lambda)$$
$$\times(2\pi)^4\delta^{(4)}(P+q-P_h-P_X)d\Gamma_{l'}d\Gamma_{P_h}$$
$$=\frac{4\pi e^4}{Q^4}L_{\mu\nu}\langle W^{\mu\nu}\rangle, \tag{4.8}$$

where

$$\langle W^{\mu\nu}\rangle \equiv \sum_{\lambda'\lambda}\rho(\lambda,\lambda')W^{\mu\nu}(\lambda',\lambda) \tag{4.9}$$

is the hadronic tensor of the polarized target, averaged over the target spin states with the spin density matrix, see Eq. (3.7).

The phase-space element of the final lepton, Eq. (4.3), can be expressed as a differential in the invariants $x_A$ and $Q^2$, and in the azimuthal angle of the final lepton around the initial lepton momentum direction in the target rest frame, $\psi_{l'}$, defined with regard to a reference direction perpendicular to the initial lepton momentum; the calculations are identical to those in unpolarized SIDIS and need not be repeated here [54]. Altogether the differential cross section is obtained as

$$d\sigma = \frac{2\pi\alpha_{\rm em}^2 y^2}{Q^6}\,dx_A dQ^2\frac{d\psi_{l'}}{2\pi}\,L_{\mu\nu}\langle W^{\mu\nu}\rangle\,d\Gamma_{P_h}, \tag{4.10}$$

where $\alpha_{\rm em}=e^2/(4\pi)\approx 1/137$ is the electromagnetic fine structure constant. The form of Eq. (4.10) separates the kinematic variables determined by the final lepton (which are the same as in inclusive scattering) from the variables characterizing the hadronic final state.

### B. Semi-inclusive structure functions

The semi-inclusive hadronic tensor Eq. (4.9) has a rich structure, in which the target polarization in the initial state is entangled with the hadron momentum in the final state. It can be expanded in kinematic tensors formed from the four-vectors of the scattering process (see Sec. II B), multiplied by the invariant polarization parameters characterizing the target polarization (see Sec. III B). The contraction of these kinematic tensors with the leptonic tensor then determines the $y$ and $\phi_h$ dependence of the cross section. The invariant polarization parameters accompanying the structures determine the target spin dependence. The invariant coefficients in this expansion are the polarized semi-inclusive structure functions, which describe the dynamics of the scattering process. We now perform this expansion, determine the independent structures, and exhibit the kinematic dependences of the cross section.

In the first step, we enumerate the possible kinematic tensors that can appear in the expansion of the hadronic tensor. The kinematic tensors must obey the transversality conditions on the hadronic tensor,

$$q_\mu\langle W^{\mu\nu}\rangle = 0, \quad \langle W^{\mu\nu}\rangle q_\nu = 0. \tag{4.11}$$

In addition, they must satisfy the Hermiticity conditions

$$\langle W^{\{\mu\nu\}}\rangle \text{ real}, \quad \langle W^{[\mu\nu]}\rangle \text{ imaginary}, \tag{4.12}$$

which follow from the fact that the symmetric (antisymmetric) part of the leptonic tensor Eq. (4.5b) is real (imaginary) and must produce a real number upon contraction with the hadronic tensor. It is natural to build the kinematic tensors from the longitudinal basis vectors of Set I, Eq. (2.6), for which the transversality conditions Eq. (4.11) take a simple form, and from the transverse basis vectors aligned with the hadron momentum, Eq. (2.15). We obtain nine kinematic tensors of different symmetry and parity:

(1) four symmetric tensors:

$$\mathcal{A}_L^{\mu\nu}=\tfrac{1}{2}e_L^\mu e_L^\nu, \quad \mathcal{A}_T^{\mu\nu}=\tfrac{1}{2}\big(e_{x'}^\mu e_{x'}^\nu+e_{y'}^\mu e_{y'}^\nu\big),$$
$$\mathcal{A}_{LT}^{\mu\nu}=-\tfrac{1}{2}e_L^{\{\mu}e_{x'}^{\nu\}}, \quad \mathcal{A}_{TT}^{\mu\nu}=\tfrac{1}{2}\big(e_{x'}^\mu e_{x'}^\nu-e_{y'}^\mu e_{y'}^\nu\big); \tag{4.13}$$

(2) one antisymmetric tensor:

$$\mathcal{A}_{LT'}^{\mu\nu}=\frac{i}{2}\epsilon^{\mu\nu\rho\sigma}e_{q,\rho}e_{y',\sigma}=\frac{i}{2}e_L^{[\mu}e_{x'}^{\nu]}; \tag{4.14}$$

(3) two symmetric pseudotensors:

$$\mathcal{A}_{LT''}^{\mu\nu}=-\tfrac{1}{2}e_L^{\{\mu}e_{y'}^{\nu\}}, \quad \mathcal{A}_{TT'}^{\mu\nu}=+\tfrac{1}{2}e_{x'}^{\{\mu}e_{y'}^{\nu\}}; \tag{4.15}$$

(4) two antisymmetric pseudotensors:

$$\mathcal{A}_{LT'''}^{\mu\nu}=\frac{i}{2}\epsilon^{\mu\nu\rho\sigma}e_{q,\rho}e_{x',\sigma}=-\frac{i}{2}e_L^{[\mu}e_{y'}^{\nu]},$$
$$\mathcal{A}_{TT''}^{\mu\nu}=-\frac{i}{2}\epsilon^{\mu\nu\rho\sigma}e_{q,\rho}e_{L,\sigma}=\frac{i}{2}e_{x'}^{[\mu}e_{y'}^{\nu]}. \tag{4.16}$$

The symmetric tensors will combine with the unpolarized part of the leptonic tensor; the antisymmetric tensors will combine with the polarized part.

In the next step, we multiply the kinematic tensors with the invariant polarization parameters representing the possible dependencies on the target polarization arising from the average with the density matrix. The available parameters are unity (no polarization) and the three vector- and five tensor-polarized parameters of Eq. (3.12), whose parity is given in Eq. (3.14). Altogether, we have as possible parameters five scalars:

(1) one unpolarized: 1 (unity);
(2) one vector-polarized: $S_T\sin(\phi_h-\phi_S)$;
(3) three tensor-polarized: $T_{LL}$, $T_{LT}\cos(\phi_h-\phi_{T_L})$, $T_{TT}\cos(2\phi_h-2\phi_{T_T})$;

and four pseudoscalars:

(1) two vector-polarized: $S_L$, $S_T\cos(\phi_h-\phi_S)$;
(2) two tensor-polarized: $T_{LT}\sin(\phi_h-\phi_{T_L})$, $T_{TT}\sin(2\phi_h-2\phi_{T_T})$.

When multiplying these parameters with the kinematic tensors we must take into account the condition of overall parity,

$$\langle W^{\mu\nu}\rangle = \text{ true tensor (parity-even)}. \tag{4.17}$$

So the parity-even kinematic tensors in Eqs. (4.13) and (4.14) can only be multiplied with the scalar parameters, while the parity-odd kinematic tensors in Eqs. (4.15) and (4.16) can only be multiplied with the pseudoscalar parameters.

Altogether this results in

$$5 \times 5 + 4 \times 4 = 41$$

independent structures in the polarized hadronic tensor.

Each independent structure is multiplied by a structure function describing the dynamical content. We use the following notation:

$$\begin{aligned} & F^{[\text{azimuthal}]}_{[\text{beam}][\text{target}],[\text{photon}]} \\ \text{beam} &= U, L \\ \text{target} &= U, S_L, S_T, T_{LL}, T_{LT}, T_{TT} \\ \text{photon} &= L, T \\ \text{azimuthal} &= 1, \cos(n\phi_h \pm \phi_i), \sin(n\phi_h \pm \phi_i). \end{aligned} \tag{4.18}$$

The labels anticipate properties of the terms in the cross section that will appear after contraction with the leptonic tensor (see below). The label *beam* refers to the dependence on the lepton helicity (symmetric or antisymmetric part of the hadronic tensor); *target* refers to the dependence on the target polarization (polarization parameters in hadronic tensor); *photon* denotes the polarization of the virtual photon (longitudinal or transverse part of the hadronic tensor); and *azimuthal* refers to the dependence on the hadron azimuthal angle $\phi_h$ that appears after contraction with the leptonic tensor. The structure functions depend on four kinematic variables: the invariant DIS variables $x_A$ and $Q^2$, Eq. (2.4); the invariant modulus of the final-state hadron transverse momentum $|\boldsymbol{P}_{hT}|$, Eq. (2.24); and one variable characterizing the longitudinal momentum, e.g., $\zeta_h$ or $\eta_h$, Eqs. (2.32a) or (2.32b) (see Sec. II D),

$$F \equiv F(x_A, Q^2; \zeta_h, |\boldsymbol{P}_{hT}|). \tag{4.19}$$

The dependence of the cross section on $\phi_h$ is explicit and follows from the decomposition of the hadronic tensor (see below).

We can now enumerate the 41 possible structures in the polarized hadronic tensor Eq. (4.9), including their structure functions. They are as follows:

(1) four with lepton unpolarized, target unpolarized:

$$F_{UU,L}\mathcal{A}^{\mu\nu}_{L}, \quad F_{UU,T}\mathcal{A}^{\mu\nu}_{T}, \quad F^{\cos\phi_h}_{UU}\mathcal{A}^{\mu\nu}_{LT}, \quad F^{\cos 2\phi_h}_{UU}\mathcal{A}^{\mu\nu}_{TT}; \tag{4.20}$$

(2) one with lepton polarized, target unpolarized:

$$F^{\sin\phi_h}_{LU}\mathcal{A}^{\mu\nu}_{LT'}; \tag{4.21}$$

(3) two with lepton unpolarized, target vector-polarized longitudinally:

$$S_L F^{\sin\phi_h}_{US_L}\mathcal{A}^{\mu\nu}_{LT''}, \quad S_L F^{\sin 2\phi_h}_{US_L}\mathcal{A}^{\mu\nu}_{TT'}; \tag{4.22}$$

(4) two with lepton polarized, target vector-polarized longitudinally:

$$S_L F_{LS_L}\mathcal{A}^{\mu\nu}_{TT''}, \quad S_L F^{\cos\phi_h}_{LS_L}\mathcal{A}^{\mu\nu}_{LT'''}; \tag{4.23}$$

(5) six with lepton unpolarized, target vector-polarized transversely:

$$\begin{aligned} & S_T \sin(\phi_h - \phi_S) F^{\sin(\phi_h-\phi_S)}_{US_T,L}\mathcal{A}^{\mu\nu}_{L}, \\ & S_T \sin(\phi_h - \phi_S) F^{\sin(\phi_h-\phi_S)}_{US_T,T}\mathcal{A}^{\mu\nu}_{T}, \\ & S_T F^{\sin(\phi_h+\phi_S)}_{US_T}\big[\cos(\phi_h - \phi_S)\mathcal{A}^{\mu\nu}_{TT'} - \sin(\phi_h - \phi_S)\mathcal{A}^{\mu\nu}_{TT}\big], \\ & S_T F^{\sin(3\phi_h-\phi_S)}_{US_T}\big[\cos(\phi_h - \phi_S)\mathcal{A}^{\mu\nu}_{TT'} + \sin(\phi_h - \phi_S)\mathcal{A}^{\mu\nu}_{TT}\big], \\ & S_T F^{\sin\phi_S}_{US_T}\big[\cos(\phi_h - \phi_S)\mathcal{A}^{\mu\nu}_{LT''} - \sin(\phi_h - \phi_S)\mathcal{A}^{\mu\nu}_{LT}\big], \\ & S_T F^{\sin(2\phi_h-\phi_S)}_{US_T}\big[\cos(\phi_h - \phi_S)\mathcal{A}^{\mu\nu}_{LT''} + \sin(\phi_h - \phi_S)\mathcal{A}^{\mu\nu}_{LT}\big]; \end{aligned} \tag{4.24}$$

(6) three with lepton polarized, target vector-polarized transversely:

$$\begin{aligned} & S_T \cos(\phi_h - \phi_S) F^{\cos(\phi_h-\phi_S)}_{LS_T}\mathcal{A}^{\mu\nu}_{TT''}, \\ & S_T F^{\cos\phi_S}_{LS_T}\big[\cos(\phi_h - \phi_S)\mathcal{A}^{\mu\nu}_{LT'''} + \sin(\phi_h - \phi_S)\mathcal{A}^{\mu\nu}_{LT'}\big], \\ & S_T F^{\cos(2\phi_h-\phi_S)}_{LS_T}\big[\cos(\phi_h - \phi_S)\mathcal{A}^{\mu\nu}_{LT'''} - \sin(\phi_h - \phi_S)\mathcal{A}^{\mu\nu}_{LT'}\big]; \end{aligned} \tag{4.25}$$

(7) four with lepton unpolarized, target tensor-polarized longitudinally:

$$T_{LL}F_{UT_{LL},L}\mathcal{A}^{\mu\nu}_{L}, \quad T_{LL}F_{UT_{LL},T}\mathcal{A}^{\mu\nu}_{T}, \quad T_{LL}F^{\cos\phi_h}_{UT_{LL}}\mathcal{A}^{\mu\nu}_{LT}, \quad T_{LL}F^{\cos 2\phi_h}_{UT_{LL}}\mathcal{A}^{\mu\nu}_{TT}; \tag{4.26}$$

(8) one with lepton polarized, target tensor-polarized longitudinally:

$$T_{LL}F^{\sin\phi_h}_{LT_{LL}}\mathcal{A}^{\mu\nu}_{LT'}; \tag{4.27}$$

(9) six with lepton unpolarized, target tensor-polarized longitudinal-transversely:

$$
\begin{aligned}
&T_{LT}\cos(\phi_h-\phi_{T_L})F_{UT_{LT},L}^{\cos(\phi_h-\phi_{T_L})}\mathcal{A}_L^{\mu\nu},\\
&T_{LT}\cos(\phi_h-\phi_{T_L})F_{UT_{LT},T}^{\cos(\phi_h-\phi_{T_L})}\mathcal{A}_T^{\mu\nu},\\
&T_{LT}F_{UT_{LT}}^{\cos(\phi_h+\phi_{T_L})}\big[\cos(\phi_h-\phi_{T_L})\mathcal{A}_{TT}^{\mu\nu}+\sin(\phi_h-\phi_{T_L})\mathcal{A}_{TT'}^{\mu\nu}\big],\\
&T_{LT}F_{UT_{LT}}^{\cos(3\phi_h-\phi_{T_L})}\big[\cos(\phi_h-\phi_{T_L})\mathcal{A}_{TT}^{\mu\nu}-\sin(\phi_h-\phi_{T_L})\mathcal{A}_{TT'}^{\mu\nu}\big],\\
&T_{LT}F_{UT_{LT}}^{\cos\phi_{T_L}}\big[\cos(\phi_h-\phi_{T_L})\mathcal{A}_{LT}^{\mu\nu}+\sin(\phi_h-\phi_{T_L})\mathcal{A}_{LT''}^{\mu\nu}\big],\\
&T_{LT}F_{UT_{LT}}^{\cos(2\phi_h-\phi_{T_L})}\big[\cos(\phi_h-\phi_{T_L})\mathcal{A}_{LT}^{\mu\nu}-\sin(\phi_h-\phi_{T_L})\mathcal{A}_{LT''}^{\mu\nu}\big];
\end{aligned}
\tag{4.28}
$$

(10) three with lepton polarized, target tensor-polarized longitudinal-transversely:

$$
\begin{aligned}
&T_{LT}\sin(\phi_h-\phi_{T_L})F_{LT_{LT}}^{\sin(\phi_h-\phi_{T_L})}\mathcal{A}_{TT''}^{\mu\nu},\\
&T_{LT}F_{LT_{LT}}^{\sin\phi_{T_L}}\big[\cos(\phi_h-\phi_{T_L})\mathcal{A}_{LT'}^{\mu\nu}-\sin(\phi_h-\phi_{T_L})\mathcal{A}_{LT'''}^{\mu\nu}\big],\\
&T_{LT}F_{LT_{LT}}^{\sin(2\phi_h-\phi_{T_L})}\big[\cos(\phi_h-\phi_{T_L})\mathcal{A}_{LT'}^{\mu\nu}+\sin(\phi_h-\phi_{T_L})\mathcal{A}_{LT'''}^{\mu\nu}\big];
\end{aligned}
\tag{4.29}
$$

(11) six with lepton unpolarized, target tensor-polarized transversely:

$$
\begin{aligned}
&T_{TT}\cos(2\phi_h-2\phi_{T_T})F_{UT_{TT},L}^{\cos(2\phi_h-2\phi_{T_T})}\mathcal{A}_L^{\mu\nu},\\
&T_{TT}\cos(2\phi_h-2\phi_{T_T})F_{UT_{TT},T}^{\cos(2\phi_h-2\phi_{T_T})}\mathcal{A}_T^{\mu\nu},\\
&T_{TT}F_{UT_{TT}}^{\cos 2\phi_{T_T}}\big[\cos(2\phi_h-2\phi_{T_T})\mathcal{A}_{TT}^{\mu\nu}+\sin(2\phi_h-2\phi_{T_T})\mathcal{A}_{TT'}^{\mu\nu}\big],\\
&T_{TT}F_{UT_{TT}}^{\cos(4\phi_h-2\phi_{T_T})}\big[\cos(2\phi_h-2\phi_{T_T})\mathcal{A}_{TT}^{\mu\nu}-\sin(2\phi_h-2\phi_{T_T})\mathcal{A}_{TT'}^{\mu\nu}\big],\\
&T_{TT}F_{UT_{TT}}^{\cos(\phi_h-2\phi_{T_T})}\big[\cos(2\phi_h-2\phi_{T_T})\mathcal{A}_{LT}^{\mu\nu}+\sin(2\phi_h-2\phi_{T_T})\mathcal{A}_{LT''}^{\mu\nu}\big],\\
&T_{TT}F_{UT_{TT}}^{\cos(3\phi_h-2\phi_{T_T})}\big[\cos(2\phi_h-2\phi_{T_T})\mathcal{A}_{LT}^{\mu\nu}-\sin(2\phi_h-2\phi_{T_T})\mathcal{A}_{LT''}^{\mu\nu}\big];
\end{aligned}
\tag{4.30}
$$

(12) three with lepton polarized, target tensor-polarized transversely:

$$
\begin{aligned}
&T_{TT}\sin(2\phi_h-2\phi_{T_T})F_{LT_{TT}}^{\sin(2\phi_h-2\phi_{T_T})}\mathcal{A}_{TT''}^{\mu\nu},\\
&T_{TT}F_{LT_{TT}}^{\sin(\phi_h-2\phi_{T_T})}\big[\sin(2\phi_h-2\phi_{T_T})\mathcal{A}_{LT'''}^{\mu\nu}-\cos(2\phi_h-2\phi_{T_T})\mathcal{A}_{LT'}^{\mu\nu}\big],\\
&T_{TT}F_{LT_{TT}}^{\sin(3\phi_h-2\phi_{T_T})}\big[\sin(2\phi_h-2\phi_{T_T})\mathcal{A}_{LT'''}^{\mu\nu}+\cos(2\phi_h-2\phi_{T_T})\mathcal{A}_{LT'}^{\mu\nu}\big].
\end{aligned}
\tag{4.31}
$$

The first 18 structure functions (target unpolarized and vector-polarized) also appear in SIDIS on a spin-1/2 target [53–56]; the last 23 (target tensor-polarized) are unique to the spin-1 case.

An alternative derivation of the independent structures can be performed by projecting the hadronic tensor on photon helicity states and using the symmetry properties of helicity amplitudes; see Appendix C. It confirms the number of 41 independent structures and provides explicit expressions of the structure functions in terms of helicity amplitudes.

In the last step, we contract the independent structures in the hadronic tensor with the leptonic tensor Eq. (4.5b). This produces the independent scalar terms in the cross section with a definite $\phi_h$ dependence. It is useful to introduce the parameter describing the ratio of longitudinal to transverse polarization of the virtual photon,

$$
\epsilon \equiv \frac{g_L^{\mu\nu}L_{\mu\nu}}{-g_T^{\mu\nu}L_{\mu\nu}} = \frac{e_L^\mu e_L^\nu L_{\mu\nu}}{\big(e_L^\mu e_L^\nu - g^{\mu\nu}\big)L_{\mu\nu}} = \frac{e_L^\mu e_L^\nu L_{\mu\nu}}{\big(e_{x'}^\mu e_{x'}^\nu + e_{y'}^\mu e_{y'}^\nu\big)L_{\mu\nu}},
\tag{4.32}
$$

which is expressed in terms of the scaling variables as

$$
\epsilon = \frac{1-y-\gamma^2y^2/4}{1-y+y^2/2+\gamma^2y^2/4}.
\tag{4.33}
$$

The contractions with the initial lepton momentum are then evaluated using the relations

$$
e_L\cdot l = \frac{Q}{2}\sqrt{\frac{1+\epsilon}{1-\epsilon}},
\tag{4.34a}
$$

$$
(e_{x'}\cdot l)^2+(e_{y'}\cdot l)^2 = -l_T^2 = \frac{Q^2}{2}\frac{\epsilon}{1-\epsilon},
\tag{4.34b}
$$

$$
\begin{aligned}
e_{x'}\cdot l &= -\sqrt{-l_T^2}\cos\phi_h\\
&= -\frac{Q}{2}\sqrt{\frac{2\epsilon}{1-\epsilon}}\cos\phi_h,
\end{aligned}
\tag{4.34c}
$$

$$e_{y'} \cdot l = -\sqrt{-l_T^2}\,\sin\phi_h = -\frac{Q}{2}\sqrt{\frac{2\epsilon}{1-\epsilon}}\,\sin\phi_h; \quad (4.34d)$$

the last two relations follow from Eqs. (2.14), (2.15), and (2.16). The contraction of the leptonic tensor with the nine kinematic tensors of Eqs. (4.13)–(4.16) gives

$$L_{\mu\nu}\mathcal{A}_L^{\mu\nu} = \frac{Q^2}{1-\epsilon}\epsilon, \quad (4.35a)$$

$$L_{\mu\nu}\mathcal{A}_T^{\mu\nu} = \frac{Q^2}{1-\epsilon}, \quad (4.35b)$$

$$L_{\mu\nu}\mathcal{A}_{TT''}^{\mu\nu} = \frac{Q^2}{1-\epsilon}\lambda_e\sqrt{1-\epsilon^2}, \quad (4.35c)$$

$$L_{\mu\nu}\mathcal{A}_{LT}^{\mu\nu} = \frac{Q^2}{1-\epsilon}\sqrt{2\epsilon(1+\epsilon)}\cos\phi_h, \quad (4.35d)$$

$$L_{\mu\nu}\mathcal{A}_{LT''}^{\mu\nu} = \frac{Q^2}{1-\epsilon}\sqrt{2\epsilon(1+\epsilon)}\sin\phi_h, \quad (4.35e)$$

$$L_{\mu\nu}\mathcal{A}_{TT}^{\mu\nu} = \frac{Q^2}{1-\epsilon}\epsilon\cos 2\phi_h, \quad (4.35f)$$

$$L_{\mu\nu}\mathcal{A}_{TT'}^{\mu\nu} = \frac{Q^2}{1-\epsilon}\epsilon\sin 2\phi_h, \quad (4.35g)$$

$$L_{\mu\nu}\mathcal{A}_{LT'''}^{\mu\nu} = \frac{Q^2}{1-\epsilon}\lambda_e\sqrt{2\epsilon(1-\epsilon)}\cos\phi_h, \quad (4.35h)$$

$$L_{\mu\nu}\mathcal{A}_{LT'}^{\mu\nu} = \frac{Q^2}{1-\epsilon}\lambda_e\sqrt{2\epsilon(1-\epsilon)}\sin\phi_h. \quad (4.35i)$$

Using these expressions we can compute the contraction of the 41 independent tensor structures in the hadronic tensor and assemble the terms in the cross section.

### C. Semi-inclusive cross section

We are now ready to write down the complete differential cross section for semi-inclusive scattering on a polarized spin-1 target, with the 41 independent structures identified above. We write it in the form

$$d\sigma = \frac{2\pi\alpha_{\rm em}^2 y^2}{Q^4(1-\epsilon)}\,dx_A dQ^2\frac{d\psi_{l'}}{2\pi} \times (\mathcal{F}_U + \mathcal{F}_S + \mathcal{F}_T)\,d\Gamma_{P_h}, \quad (4.36)$$

where $\mathcal{F}_{U,S,T}$ contain the terms with a given dependence on the target polarization (unpolarized, vector polarized, tensor polarized). The terms independent of the target polarization are

$$\begin{aligned}\mathcal{F}_U =& F_{UU,T} + \epsilon F_{UU,L} \\ &+ \sqrt{2\epsilon(1+\epsilon)}\cos\phi_h F_{UU}^{\cos\phi_h} \\ &+ \epsilon\cos 2\phi_h F_{UU}^{\cos 2\phi_h} \\ &+ (2\lambda_e)\sqrt{2\epsilon(1-\epsilon)}\sin\phi_h F_{LU}^{\sin\phi_h}. \end{aligned} \quad (4.37)$$

The terms dependent on the vector polarization are

$$\begin{aligned}\mathcal{F}_S =& S_L\big[\sqrt{2\epsilon(1+\epsilon)}\sin\phi_h F_{US_L}^{\sin\phi_h} + \epsilon\sin 2\phi_h F_{US_L}^{\sin 2\phi_h}\big] \\ &+ S_L(2\lambda_e)\big[\sqrt{1-\epsilon^2}F_{LS_L} + \sqrt{2\epsilon(1-\epsilon)}\cos\phi_h F_{LS_L}^{\cos\phi_h}\big] \\ &+ S_T\big[\sin(\phi_h-\phi_S)\big(F_{US_T,T}^{\sin(\phi_h-\phi_S)} + \epsilon F_{US_T,L}^{\sin(\phi_h-\phi_S)}\big) \\ &+ \epsilon\sin(\phi_h+\phi_S)F_{US_T}^{\sin(\phi_h+\phi_S)} \\ &+ \epsilon\sin(3\phi_h-\phi_S)F_{US_T}^{\sin(3\phi_h-\phi_S)} \\ &+ \sqrt{2\epsilon(1+\epsilon)}\sin\phi_S F_{US_T}^{\sin\phi_S} \\ &+ \sqrt{2\epsilon(1+\epsilon)}\sin(2\phi_h-\phi_S)F_{US_T}^{\sin(2\phi_h-\phi_S)}\big] \\ &+ S_T(2\lambda_e)\big[\sqrt{1-\epsilon^2}\cos(\phi_h-\phi_S)F_{LS_T}^{\cos(\phi_h-\phi_S)} \\ &+ \sqrt{2\epsilon(1-\epsilon)}\cos\phi_S F_{LS_T}^{\cos\phi_S} \\ &+ \sqrt{2\epsilon(1-\epsilon)}\cos(2\phi_h-\phi_S)F_{LS_T}^{\cos(2\phi_h-\phi_S)}\big]. \end{aligned} \quad (4.38)$$

The terms dependent on the tensor polarization are

$$\begin{aligned}\mathcal{F}_T =& T_{LL}\big[F_{UT_{LL},T} + \epsilon F_{UT_{LL},L} \\ &+ \sqrt{2\epsilon(1+\epsilon)}\cos\phi_h F_{UT_{LL}}^{\cos\phi_h} \\ &+ \epsilon\cos 2\phi_h F_{UT_{LL}}^{\cos 2\phi_h}\big] \\ &+ T_{LL}(2\lambda_e)\sqrt{2\epsilon(1-\epsilon)}\sin\phi_h F_{LT_{LL}}^{\sin\phi_h} \\ &+ T_{LT}\big[\cos(\phi_h-\phi_{T_L}) \\ &\times\big(F_{UT_{LT},T}^{\cos(\phi_h-\phi_{T_L})} + \epsilon F_{UT_{LT},L}^{\cos(\phi_h-\phi_{T_L})}\big) \\ &+ \epsilon\cos(\phi_h+\phi_{T_L})F_{UT_{LT}}^{\cos(\phi_h+\phi_{T_L})} \\ &+ \epsilon\cos(3\phi_h-\phi_{T_L})F_{UT_{LT}}^{\cos(3\phi_h-\phi_{T_L})} \\ &+ \sqrt{2\epsilon(1+\epsilon)}\cos\phi_{T_L}F_{UT_{LT}}^{\cos\phi_{T_L}} \\ &+ \sqrt{2\epsilon(1+\epsilon)}\cos(2\phi_h-\phi_{T_L})F_{UT_{LT}}^{\cos(2\phi_h-\phi_{T_L})}\big] \\ &+ T_{LT}(2\lambda_e)\big[\sqrt{1-\epsilon^2}\sin(\phi_h-\phi_{T_L})F_{LT_{LT}}^{\sin(\phi_h-\phi_{T_L})} \\ &+ \sqrt{2\epsilon(1-\epsilon)}\sin\phi_{T_L}F_{LT_{LT}}^{\sin\phi_{T_L}} \\ &+ \sqrt{2\epsilon(1-\epsilon)}\sin(2\phi_h-\phi_{T_L})F_{LT_{LT}}^{\sin(2\phi_h-\phi_{T_L})}\big] \\ &+ T_{TT}\big[\cos(2\phi_h-2\phi_{T_T}) \\ &\times\big(F_{UT_{TT},T}^{\cos(2\phi_h-2\phi_{T_T})} + \epsilon F_{UT_{TT},L}^{\cos(2\phi_h-2\phi_{T_T})}\big) \\ &+ \epsilon\cos 2\phi_{T_T}F_{UT_{TT}}^{\cos 2\phi_{T_T}} \\ &+ \epsilon\cos(4\phi_h-2\phi_{T_T})F_{UT_{TT}}^{\cos(4\phi_h-2\phi_{T_T})} \\ &+ \sqrt{2\epsilon(1+\epsilon)}\cos(\phi_h-2\phi_{T_T})F_{UT_{TT}}^{\cos(\phi_h-2\phi_{T_T})} \\ &+ \sqrt{2\epsilon(1+\epsilon)}\cos(3\phi_h-2\phi_{T_T})F_{UT_{TT}}^{\cos(3\phi_h-2\phi_{T_T})}\big] \\ &+ T_{TT}(2\lambda_e)\big[\sqrt{1-\epsilon^2}\sin(2\phi_h-2\phi_{T_T})F_{LT_{TT}}^{\sin(2\phi_h-2\phi_{T_T})} \\ &+ \sqrt{2\epsilon(1-\epsilon)}\sin(\phi_h-2\phi_{T_T})F_{LT_{TT}}^{\sin(\phi_h-2\phi_{T_T})} \\ &+ \sqrt{2\epsilon(1-\epsilon)}\sin(3\phi_h-2\phi_{T_T})F_{LT_{TT}}^{\sin(3\phi_h-2\phi_{T_T})}\big]. \end{aligned} \quad (4.39)$$

The decomposition predicts the dependence of the cross section on the beam and target polarization and on the azimuthal angle of the produced hadron. One observes the following:

(1) The form of the unpolarized and vector-polarized parts of the cross section for the spin-1 target is identical to that for the spin-1/2 target [54].
(2) The $\epsilon$ and $\phi_h$ dependence of the $T_{LL}$ tensor-polarized part of the cross section (both for unpolarized and polarized lepton) is identical to that of the unpolarized part.
(3) The $\epsilon$ and $\phi_h$ dependence of the $T_{LT}$ tensor-polarized part of the cross section is analogous to that of the $S_T$ vector-polarized part, only with the replacement $\sin \to \cos$ because of the different parity of the spin vector and tensor, and with the offset angle $\phi_S \to \phi_{T_L}$.
(4) The azimuthal dependence of the $T_{TT}$ tensor-polarized part of the cross section is essentially different from that of the $S_T$ vector-polarized part. The first term in the $T_{TT}$ cross section has a $\cos(2\phi_h - 2\phi_{T_T})$ dependence, in the place where the $S_T$ cross section has $\sin(\phi_h - \phi_S)$. A term with $\cos(4\phi_h - 2\phi_{T_T})$ dependence appears in the $T_{TT}$ part of the cross section, which has no counterpart in the $S_T$ part. The $4\phi_h$ dependence is absent in the spin-1/2 target and represents a unique feature of the spin-1 target.

We recall that longitudinal and transverse ($L$ and $T$) target polarization here are defined covariantly relative to the basis vectors $e_{L*}$ and $e_{x'}, e_{y'}$ [see Eq. (3.12)], which correspond to the longitudinal and transverse directions in the collinear frame. In the target rest frame this corresponds to target polarization along the $\boldsymbol{q}$-vector direction, not along the lepton beam direction.

The decomposition also predicts the dependence of the cross section on $\epsilon$, and thus the dependence on $y$ at fixed $x_A$ and $Q^2$; see Eq. (4.33). One observes that the terms proportional to the lepton helicity $\lambda_e$ involve factors $\sqrt{1-\epsilon}$, which are $\propto y$ for $y \ll 1$. This determines the dependence of beam spin asymmetries on the center-of-mass energy $s$ for fixed $x_A$ and $Q^2$ (depolarization factors).

The structures in the SIDIS cross section can be classified according to their behavior under (naive) time reversal [32,54]. The spin-1 case can be treated in analogy to the spin-1/2 case. The structures with a single-spin dependence (on the lepton helicity $\lambda_e$, or the target vector polarization $S_L$ and $S_T$) have a sine-type dependence on $\phi_h$ or $\phi_S$ and are $T$-odd; the structures with no spin dependence or double-spin dependence have a cosine-type dependence on the angles and are $T$-even. Note that only the vector polarization of the target counts as "spin dependence" for this purpose, not the tensor polarization (see also the discussion in Appendix B). The $T$-odd structures in the unpolarized and vector-polarized spin-1 cross section are the same as in the spin-1/2 cross section. In the tensor-polarized spin-1 cross section, new $T$-odd structures appear in the $\lambda_e$-dependent terms:

$$F_{LT_{LL}}^{\sin\phi_h}, F_{LT_{LT}}^{\sin(\phi_h-\phi_{T_L})}, F_{LT_{LT}}^{\sin\phi_{T_L}}, F_{LT_{LT}}^{\sin(2\phi_h-\phi_{T_L})},$$
$$F_{LT_{TT}}^{\sin(2\phi_h-2\phi_{T_T})}, F_{LT_{TT}}^{\sin(\phi_h-2\phi_{T_T})}, F_{LT_{TT}}^{\sin(3\phi_h-2\phi_{T_T})}. \quad (4.40)$$

The $T$-odd structures are special in regard to dynamics, as they require production amplitudes with nonzero phases and are sensitive to final-state interactions (see Part II [1]).

The analysis presented here assumes zero lepton mass. At this level the cross section depends only on the lepton helicity, which is conserved in the scattering process. When the finite lepton mass is included, transverse lepton polarization becomes possible, and the cross section develops single and double-spin dependent structures involving the transverse lepton spin.

The method described here can be generalized to targets of higher spin. The extra spin degrees of freedom provide additional polarization intensities and azimuthal angles, which lead to a proliferation of structures. A sketch of the procedure and the counting of the number of structures is provided in Appendix D.

The general decomposition of the spin-1 SIDIS cross section obtained here agrees with the one reported in Ref. [32]. That work uses a different normalization of the semi-inclusive structure functions and a different convention for the tensor polarization intensities; the tensor polarization angles are the same as ours. The correspondence is described in detail in Appendix E. The number of 41 independent structures also agrees with earlier results for the exclusive deuteron electrodisintegration cross section [57].

### D. Connection with inclusive scattering

The cross section for semi-inclusive scattering has a complex form, with structures arising from the interplay of the initial-state momentum and polarization variables with the final-state hadron momentum. The cross section for inclusive scattering (summation over all final-state hadrons, no measurement of final-state momenta) has a simpler form. We now establish the connection of our semi-inclusive cross-section parametrization with the standard inclusive cross-section parametrizations for the polarized spin-1 target [16].

The semi-inclusive structure functions satisfy certain "sum rules" connecting them with the inclusive structure functions [54]. They follow from longitudinal energy/momentum conservation and express the fact that the total energy/momentum of the inclusive final state is the sum of the energy/momentum carried by the hadrons counted differentially in the semi-inclusive cross section. To derive them, one assumes the following: (i) The final states in inclusive scattering are composed from members of set of distinct hadrons species $\{h\}$. (ii) The semi-inclusive cross section for a given hadron species $h$ describes the differential probability distribution for the production of such hadron in the phase-space element $d\Gamma_{P_h}$, under the condition that the scattered lepton is detected in $d\Gamma_{l'}$. (iii) The total energy/momentum of the inclusive final state can be computed by integrating over the energy/momentum distribution of each hadron species and summing over the species.

The cross section of inclusive scattering from a spin-1 target is parametrized as

$$d\sigma = \frac{2\pi\alpha_{\rm em}^2 y^2}{Q^4(1-\epsilon)}\, dx_A dQ^2 \frac{d\psi_{l'}}{2\pi}(\overline{\mathcal{F}}_U + \overline{\mathcal{F}}_S + \overline{\mathcal{F}}_T), \quad (4.41)$$

where the functions $\overline{\mathcal{F}}_U, \overline{\mathcal{F}}_S, \overline{\mathcal{F}}_T$ contain the terms with a given dependence on the target polarization (unpolarized, vector-polarized, tensor-polarized) and are expanded in products of polarization parameters and structure functions. The form of Eq. (4.41) is analogous to that of the semi-inclusive cross section Eq. (4.36).

It is convenient to formulate the sum rules in terms of the light-front momentum variables for the final hadron $h$, in which the integration measure takes the simple form Eq. (2.39) or (2.40), is independent of the hadron mass, and permits separation of the longitudinal and transverse hadron momentum variables (see Sec. II D). From the conservation of plus momentum we obtain the sum rule

$$\sum_h \int d\Gamma_{P_h}\, P_h^+\, (\mathcal{F}_U + \mathcal{F}_S + \mathcal{F}_T)_h = (P+q)^+ (\overline{\mathcal{F}}_U + \overline{\mathcal{F}}_S + \overline{\mathcal{F}}_T), \tag{4.42}$$

or

$$\begin{aligned}\sum_h \int d\Gamma_{P_h}\, \zeta_h\, (\mathcal{F}_U + \mathcal{F}_S + \mathcal{F}_T)_h &= \sum_h \frac{1}{2(2\pi)^3} \int d\zeta_h \int d^2P_{hT}\, (\mathcal{F}_U + \mathcal{F}_S + \mathcal{F}_T)_h \\ &= \overline{\mathcal{F}}_U + \overline{\mathcal{F}}_S + \overline{\mathcal{F}}_T. \end{aligned} \tag{4.43}$$

Similar sum rules are obtained from the light-front minus momentum variables; they are equivalent because of the mass shell condition on the hadron four-momentum and overall energy-momentum conservation in the scattering process.

From the cross section sum rule Eq. (4.43) we obtain relations between the individual semi-inclusive and inclusive structure functions by separating the terms with different beam and target spin dependence. When integrating the semi-inclusive functions Eqs. (4.37)–(4.39) over the hadron momentum, all terms with a harmonic azimuthal dependence on $\phi_h$ drop out because the sine and cosine functions integrate to zero over the full period $[0, 2\pi]$. In the remaining terms, the integrated semi-inclusive structure functions can be matched with the conventional inclusive structure functions. To express the relations we use the shorthand notation

$$\sum_h \int F_{[\dots]} \equiv \sum_h \frac{1}{2(2\pi)^3} \int d\zeta_h \int d^2P_{hT}\, F_{[\dots]h}. \tag{4.44}$$

For the unpolarized and vector-polarized structures we obtain

$$\sum_h \int F_{UU,L} = (1+\gamma^2)\frac{F_2}{x_A} - 2F_1, \tag{4.45a}$$

$$\sum_h \int F_{UU,T} = 2F_1, \tag{4.45b}$$

$$\sum_h \int F_{LS_L} = 2(g_1 - \gamma^2 g_2), \tag{4.45c}$$

$$\sum_h \int F_{LS_T}^{\cos\phi_S} = -2\gamma(g_1 + g_2), \tag{4.45d}$$

where $F_{1,2}$ and $g_{1,2}$ are the inclusive structure functions in the standard convention (we suppress the arguments $x_A$ and $Q^2$ for brevity). For the tensor-polarized structures we obtain

$$\begin{aligned}\sum_h \int F_{UT_{LL},L} &= \frac{1}{x_A}\Big[2(1+\gamma^2)x_A b_1 - (1+\gamma^2)^2\Big(\frac{1}{3}b_2 + b_3 + b_4\Big) \\ &\quad - (1+\gamma^2)\Big(\frac{1}{3}b_2 - b_4\Big) - \Big(\frac{1}{3}b_2 - b_3\Big)\Big], \end{aligned} \tag{4.46a}$$

$$\begin{aligned}\sum_h \int F_{UT_{LL},T} &= -\Big[2(1+\gamma^2)b_1 - \frac{\gamma^2}{x_A}\Big(\frac{1}{6}b_2 - \frac{1}{2}b_3\Big)\Big], \end{aligned} \tag{4.46b}$$

$$\begin{aligned}\sum_h \int F_{UT_{LT}}^{\cos\phi_{T_L}} &= -\frac{\gamma}{2x_A}\Big[(1+\gamma^2)\Big(\frac{1}{3}b_2 - b_4\Big) + \Big(\frac{2}{3}b_2 - 2b_3\Big)\Big], \end{aligned} \tag{4.46c}$$

$$\sum_h \int F_{UT_{TT}}^{\cos 2\phi_{T_T}} = -\frac{\gamma^2}{x_A}\Big(\frac{1}{6}b_2 - \frac{1}{2}b_3\Big), \tag{4.46d}$$

where $b_{1-4}$ are the structure functions of the inclusive cross section for a tensor-polarized spin-1 target in the convention of Ref. [16]. For reference we give here the relations between the tensors $r^{\mu\nu}, s^{\mu\nu}, r^{\mu\nu}, u^{\mu\nu}$ defined in Ref. [16] and the tensors $\mathcal{A}_i^{\mu\nu}$ used in our decomposition (note that Ref. [16] uses $\epsilon_{0123} = 1$):

$$r^{\mu\nu} = -2(1+\gamma^2)T_{LL}\big(\mathcal{A}_L^{\mu\nu} - \mathcal{A}_T^{\mu\nu}\big), \tag{4.47a}$$

$$s^{\mu\nu} = -2(1+\gamma^2)^2 T_{LL}\frac{1}{x_A}\mathcal{A}_L^{\mu\nu}, \tag{4.47b}$$

$$\begin{aligned} t^{\mu\nu} &= -(1+\gamma^2)\frac{1}{x_A}\big\{2T_{LL}\mathcal{A}_L^{\mu\nu} - \gamma T_{LT}\big[\cos(\phi_h - \phi_{T_L})\mathcal{A}_{LT}^{\mu\nu} \\ &\quad + \sin(\phi_h - \phi_{T_L})\mathcal{A}_{LT''}^{\mu\nu}\big]\big\}, \end{aligned} \tag{4.47c}$$

$$\begin{aligned} u^{\mu\nu} &= -\frac{1}{x_A}\big\{2T_{LL}\big(\mathcal{A}_L^{\mu\nu} - \gamma^2\mathcal{A}_{TT}^{\mu\nu}\big) \\ &\quad - 2\gamma T_{LT}\big[\cos(\phi_h - \phi_{T_L})\mathcal{A}_{LT}^{\mu\nu} + \sin(\phi_h - \phi_{T_L})\mathcal{A}_{LT''}^{\mu\nu}\big] \\ &\quad + \gamma^2 T_{TT}\big[\cos(2\phi_h - 2\phi_{T_T})\mathcal{A}_{TT}^{\mu\nu} \\ &\quad + \sin(2\phi_h - 2\phi_{T_T})\mathcal{A}_{TT'}^{\mu\nu}\big]\big\}. \end{aligned} \tag{4.47d}$$

A special situation arises in the $T$-odd structures without $\phi_h$ dependence in the semi-inclusive cross section. Time-reversal invariance, combined with the Hermiticity of the electromagnetic current operator, forbids $T$-odd structures in the inclusive cross section in one-photon exchange approximation [62]. This implies that the sum rule of the corresponding semi-inclusive structure functions must be zero

(see Ref. [53] for the spin-1/2 case),

$$\sum_h \int F_{US_T}^{\sin\phi_S} = 0, \tag{4.48a}$$

$$\sum_h \int F_{LT_{LT}}^{\sin\phi_{T_L}} = 0. \tag{4.48b}$$

The vanishing of these structures is not caused by averaging out of the $\phi_h$ dependence (the terms in the semi-inclusive cross section have no dependence on $\phi_h$) but represents a nontrivial dynamical constraint on the semi-inclusive structure functions, involving the dependence on the longitudinal and transverse hadron momentum. Note that the relations Eq. (4.48) are limited to the one-photon exchange approximation; at two-photon exchange level the inclusive cross section develops a transverse single-spin dependence [63].

## V. POLARIZATION OBSERVABLES

### A. Preparation of target polarization

The decomposition of the semi-inclusive differential cross section implies a definite dependence on the kinematic variables. The dependence on the beam and target polarization, the virtual photon polarization, and the final-state hadron azimuthal angle $\phi_h$ is kinematic and shown explicitly in the expressions in Sec. IV C. The dependence on the DIS variables $x_A$ and $Q^2$, and the final-state hadron longitudinal and transverse momenta, $z_h$ and $|\boldsymbol{P}_{hT}|$, is dynamical and contained in the invariant structure functions, which represent the basic independent structures characterizing the process. Observables for a defined experimental setup can be derived from the complete expressions of the differential cross section. Depending on the setup and the goals of the measurement, a large variety of observables (polarized differential cross sections, azimuthal harmonics, spin asymmetries, etc.) can be constructed and used to separate the independent structures. We now describe some basic techniques for constructing the observables and separating the structures. Specific examples will be presented for DIS on the deuteron with spectator nucleon tagging in Part II [1].

We first describe the preparation of the target polarization of the spin-1 target. We consider a setup where the spin-1 target is polarized along a fixed spatial direction in a given frame (to be specified), measurements are performed in the pure spin states with projection $\Lambda = (+1, 0, -1)$ along the axis, and then certain sums or differences of cross-section measurements in the pure spin states are taken. This scheme covers most actual experimental setups; a general setup can be modeled by superposing several such measurements. The expressions are presented in relativistically covariant form, using the covariant representation of the spin density matrix in Sec. III, and can be applied to fixed-target and colliding-beam experiments.

The polarization axis is described covariantly by a spacelike four-vector $N$ with

$$N \cdot P = 0, \quad N^2 = -1. \tag{5.1}$$

The spin density matrix of the pure spin state with spin projection $\Lambda$ on the axis $N$ is given by the general expression Eq. (3.9) with the parameters [39]

$$S^\alpha = \Lambda N^\alpha, \tag{5.2a}$$

$$T^{\alpha\beta} = \frac{1}{6} W(\Lambda) \left( g^{\alpha\beta} - \frac{P^\alpha P^\beta}{P^2} + 3 N^\alpha N^\beta \right), \tag{5.2b}$$

$$W(\Lambda) \equiv (1, -2, 1) \quad \text{for } \Lambda = (+1, 0, -1). \tag{5.2c}$$

The four-vector $N$ then can be expanded in the basis vectors of Set II, Eq. (2.7), as

$$N = -\cos\theta_N \, e_{L*} + \sin\theta_N [\cos\phi_N \, e_x - \sin\phi_N \, e_y] \tag{5.3a}$$

$$= -\cos\theta_N \, e_{L*} + \sin\theta_N [\cos(\phi_h - \phi_N) \, e_{x'} + \sin(\phi_h - \phi_N) \, e_{y'}]. \tag{5.3b}$$

Here the coefficients are expressed in terms of two angular parameters, $\theta_N$ and $\phi_N$. $\theta_N$ is defined such that, in the target rest frame, where $N = (0, \boldsymbol{N})$ and the basis vectors are given by Eqs. (2.23), (2.21), and (2.22), $\theta_N$ is the polar angle of $\boldsymbol{N}$ relative to the $z$ axis. The azimuthal angle $\phi_N$ is defined as specified for $\phi_S$ in Fig. 1. The invariant polarization parameters generated by the pure state are then computed by contracting Eq. (5.2) with the basis vectors, as specified in Eq. (3.12). We obtain

$$S_L = \Lambda \cos\theta_N, \tag{5.4a}$$

$$S_T = \Lambda \sin\theta_N, \quad \phi_S = \phi_N, \tag{5.4b}$$

$$T_{LL} = \tfrac{1}{6} W(\Lambda)(-1 + 3\cos^2\theta_N) \tag{5.4c}$$

$$T_{LT} = \tfrac{1}{2} W(\Lambda) \sin\theta_N \cos\theta_N, \quad \phi_{T_L} = \phi_N, \tag{5.4d}$$

$$T_{TT} = \tfrac{1}{2} W(\Lambda) \sin^2\theta_N, \quad \phi_{T_T} = \phi_N. \tag{5.4e}$$

One observes that all the three vector polarization parameters $\{S_L, S_T, \phi_S\}$ and the five tensor polarization parameters $\{T_{LL}, T_{LT}, T_{TT}, \phi_{T_L}, \phi_{T_T}\}$ can be assigned nontrivial values through suitable choices of the pure state polarization parameters $\{\Lambda, \theta_N, \phi_N\}$.

In most experiments the target polarization is prepared along an axis defined relative to the lepton beam direction (parallel or perpendicular to it). This includes (i) fixed-target experiments, where the lepton beam defines an axis in the target rest frame; (ii) colliding-beam experiments with head-on collisions of the lepton and nuclear beams (zero crossing angle); this situation is equivalent to fixed-target when viewed in target rest frame.

For target polarization parallel to the lepton beam axis (denoted by $\parallel$) the axis four-vector is given by

$$N = \frac{-l + (e_P \cdot l) e_P}{\sqrt{(e_P \cdot l)^2}}, \tag{5.5}$$

which in the target rest frame becomes the unit vector along the negative lepton momentum,

$$N = (0, -\boldsymbol{l}/|\boldsymbol{l}|). \tag{5.6}$$

The polarization is thus measured relative to the lepton beam axis in the target rest frame, with $\Lambda = +1(-1)$ corresponding to polarization opposite (along) the lepton momentum (see

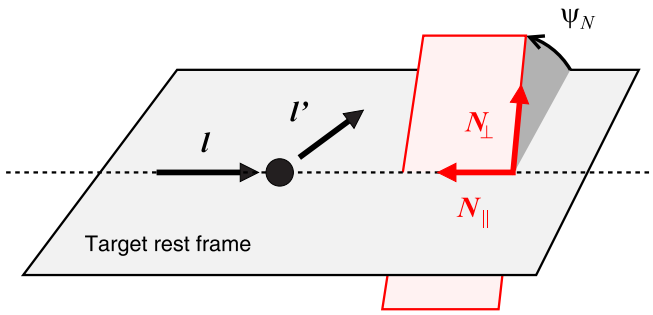



FIG. 2. Target polarization relative to the lepton beam axis in the target rest frame. Shown are the spatial components of the vector $\boldsymbol{N}$ in the target rest frame. For parallel polarization ($\parallel$), $\boldsymbol{N}$ points in the direction opposite to the initial lepton momentum. For perpendicular polarization ($\perp$), the angle $\psi_N$ is measured from the plane spanned by the final lepton momentum in the sense as indicated.

Fig. 2). For this choice of polarization axis the coefficients in Eq. (5.3) are

$$\cos\theta_N = \frac{1+\gamma^2 y/2}{\sqrt{1+\gamma^2}}, \tag{5.7a}$$

$$\sin\theta_N = \frac{\gamma\sqrt{1-y-\gamma^2y^2/4}}{\sqrt{1+\gamma^2}}, \quad \phi_N = 0. \tag{5.7b}$$

For target polarization perpendicular to the lepton beam axis (denoted by $\perp$) the axis four-vector is given by

$$N = \cos\psi_N\, e_\perp - \sin\psi_N\, e_y, \tag{5.8a}$$

$$e_\perp^\alpha \equiv \frac{\epsilon^{\alpha\beta\gamma\delta} e_{P,\beta} e_{y,\gamma} l_\delta}{\sqrt{(e_P\cdot l)^2}} = \frac{(e_x\cdot l)e_{L*}^\alpha - (e_{L*}\cdot l)e_x^\alpha}{\sqrt{(e_x\cdot l)^2+(e_{L*}\cdot l)^2}}, \tag{5.8b}$$

$$e_P\cdot e_\perp,\ e_y\cdot e_\perp,\ e_\perp\cdot l = 0, \tag{5.8c}$$

which in the target rest frame becomes

$$N = (0,\boldsymbol{N}), \quad \boldsymbol{N} = \cos\psi_N \boldsymbol{e}_\perp - \sin\psi_N \boldsymbol{e}_y, \tag{5.9a}$$

$$\boldsymbol{e}_\perp \equiv -\boldsymbol{e}_y \times \frac{\boldsymbol{l}}{|\boldsymbol{l}|} = \frac{l^x \boldsymbol{e}_z - l^z \boldsymbol{e}_x}{|\boldsymbol{l}|}. \tag{5.9b}$$

In the last expression, $\boldsymbol{e}_z$ and $\boldsymbol{e}_x$ are the three-dimensional components of the basis vectors in the target rest frame as defined in Sec. II B, and $l^z$ and $l^x$ are the components of $\boldsymbol{l}$ along these vectors. $\boldsymbol{e}_\perp$ is the unit vector in the lepton scattering plane perpendicular to $\boldsymbol{l}$, such that $\{\boldsymbol{e}_\perp, \boldsymbol{e}_y, -\boldsymbol{l}/|\boldsymbol{l}|\}$ form a right-handed system (see Fig. 2). For this choice of polarization axis the coefficients in Eq. (5.3) are

$$\cos\theta_N = \frac{\gamma\sqrt{1-y-\gamma^2y^2/4}}{\sqrt{1+\gamma^2}}\cos\psi_N, \tag{5.10a}$$

$$\sin\theta_N\cos\phi_N = \frac{1+\gamma^2 y/2}{\sqrt{1+\gamma^2}}\cos\psi_N, \tag{5.10b}$$

$$\sin\theta_N\sin\phi_N = \sin\psi_N. \tag{5.10c}$$

Note that the definition of the angle $\psi_N$ in Eq. (5.8a) and Fig. 2 differs from Ref. [39] (see Appendix A). Using the above expressions one can easily compute the invariant polarization parameters for a given experimental setup in fixed-target or colliding-beam experiments.

### B. Separation of spin structures

Equation (5.4) gives the values of the invariant polarization parameters in pure spin states with polarization axis $N$ and spin projection $\Lambda$. The parts of the cross section proportional to these parameters then can be separated by performing measurements in pure spin states with different $\Lambda$ and taking sums/differences.

(i) The unpolarized part of the cross section is obtained by performing measurements in all three spin states and summing them,

$$U: \quad \sigma(\Lambda=+1)+\sigma(\Lambda=-1)+\sigma(\Lambda=0). \tag{5.11}$$

The summation over all three states sets both vector and tensor polarization to zero, because $W(+1)+W(0)+W(-1)=0$. Note that the summation over only the $\Lambda=\pm1$ states has nonzero tensor polarization, because $W(+1)+W(-1)=2\neq 0$. The $\Lambda=0$ state is thus needed for unpolarized measurements.

(ii) The vector-polarized part of the cross section is isolated by taking the difference of measurements in spin states with $\Lambda=\pm1$,

$$S: \quad \sigma(\Lambda=+1)-\sigma(\Lambda=-1). \tag{5.12}$$

In the difference the values of $S_L$ and $S_T$ add up, while the values of $T_{LL}$, $T_{LT}$, and $T_{TT}$ sum to zero; see Eq. (5.4). The $\Lambda=0$ state is not needed for measurements of vector-polarized structures. Longitudinal and transverse polarization can be selected by choosing $\theta_N=0$ and $\pi/2$, respectively.

(iii) The tensor-polarized part of the cross section is isolated by performing measurements in all three spin states and taking the combination

$$T: \quad \sigma(\Lambda=+1)+\sigma(\Lambda=-1)-2\sigma(\Lambda=0). \tag{5.13}$$

The combination removes the unpolarized and vector-polarized terms. The values of $\{T_{LL}, T_{LT}, T_{TT}\}$ can be assigned by choosing appropriate angles of the pure-state polarization axis; see Eq. (5.4). Special choices are

| $\cos\theta_N$ | $T_{LL}$ | $T_{LT}$ | $T_{TT}$ |
|---|---|---|---|
| $\pm1$ | ✓ | 0 | 0 |
| $\pm\frac{1}{\sqrt{3}}$ | 0 | ✓ | ✓ |
| 0 | ✓ | 0 | ✓ |

(5.14)

Using suitable combinations of measurements with these special axis angles one can separate the various tensor-polarized structures.

The preparation of the spin density matrix of the spin-1 target as a superposition of pure states quantized along certain directions practiced here is analogous to the preparation of photon polarization in optics [60]. The polarization parameters can be associated with probability differences (intensity differences) measured along certain polarization directions. Measurements along several directions, including relative angles other than 90°, are needed to completely specify the polarization of the spin-1 system; see Eq. (5.14).

### C. Azimuthal angle dependence

The dependence of the differential cross section on the hadron azimuthal angle $\phi_h$ and the polarization angles $\phi_S, \phi_{T_L}, \phi_{T_T}$ is explicit and described by simple trigonometric functions; see Eqs. (4.37)–(4.39). The individual structure functions can be extracted by measuring the azimuthal dependence of the differential cross section and computing certain averages weighted with trigonometric functions. We use the notation

$$\langle \mathcal{F} \rangle_w \equiv \frac{\int_0^{2\pi} \frac{d\phi_h}{2\pi}\, w(\phi_h)\, \mathcal{F}(\phi_h)}{\int_0^{2\pi} \frac{d\phi_h}{2\pi}\, [w(\phi_h)]^2}, \tag{5.15a}$$

$$w(\phi_h, \phi_{\rm pol}) \equiv 1, \cos(n\phi_h), \sin(n\phi_h) \quad (n = 1\text{–}4). \tag{5.15b}$$

The averages can be computed by using the addition theorems of the trigonometric functions to separate the dependencies on $\phi_h$ and $\phi_S$, $\phi_{T_L}, \phi_{T_T}$ in the various terms in Eqs. (4.37)–(4.39) and using the orthogonality properties of the elementary trigonometric functions in $n\phi_h$. The $\phi_h$-independent differential cross section (average with $h = 1$) is given by Eq. (4.36) with

$$\begin{aligned}\langle \mathcal{F} \rangle_1 &= \int_0^{2\pi} \frac{d\phi_h}{2\pi}\, \mathcal{F} \\ &= F_{UU,T} + \epsilon F_{UU,L} + S_L(2\lambda_e)\sqrt{1-\epsilon^2}F_{LS_L} \\ &\quad + S_T(2\lambda_e)\sqrt{2\epsilon(1-\epsilon)}\cos\phi_S F_{LS_T}^{\cos\phi_S} \\ &\quad + T_{LL}(F_{UT_{LL},T} + \epsilon F_{UT_{LL},L}) \\ &\quad + T_{LT}\sqrt{2\epsilon(1+\epsilon)}\cos\phi_{T_L} F_{UT_{LT}}^{\cos\phi_{T_L}} \\ &\quad + T_{LT}(2\lambda_e)\sqrt{2\epsilon(1-\epsilon)}\sin\phi_{T_L} F_{LT_{LT}}^{\sin\phi_{T_L}} \\ &\quad + T_{TT}\epsilon\cos 2\phi_{T_T} F_{UT_{TT}}^{\cos 2\phi_{T_T}}. \end{aligned} \tag{5.16}$$

The averages with $n = 0$, 1, and 2 generally have terms with all the spin dependencies present in the cross section, because spin-orbit effects in the SIDIS process mix the azimuthal and spin dependence of the structures.

The averages with $n = 3$ and 4 have fewer terms and are of particular interest. The $n = 3$ averages are

$$\begin{aligned}\langle \mathcal{F} \rangle_{\cos 3\phi_h} &= -S_T\epsilon\sin\phi_S F_{US_T}^{\sin(3\phi_h-\phi_S)} \\ &\quad + T_{LT}\epsilon\cos(\phi_{T_L}) F_{UT_{LT}}^{\cos(3\phi_h-\phi_{T_L})} \\ &\quad + T_{TT}\sqrt{2\epsilon(1+\epsilon)}\cos(2\phi_{T_T}) F_{UT_{TT}}^{\cos(3\phi_h-2\phi_{T_T})} \\ &\quad - T_{TT}(2\lambda_e)\sqrt{2\epsilon(1-\epsilon)}\sin(2\phi_{T_T}) F_{LT_{TT}}^{\sin(3\phi_h-2\phi_{T_T})}, \end{aligned} \tag{5.17a}$$

$$\begin{aligned}\langle \mathcal{F} \rangle_{\sin 3\phi_h} &= S_T\epsilon\cos\phi_S F_{US_T}^{\sin(3\phi_h-\phi_S)} \\ &\quad + T_{LT}\epsilon\sin(\phi_{T_L}) F_{UT_{LT}}^{\cos(3\phi_h-\phi_{T_L})} \\ &\quad + T_{TT}\sqrt{2\epsilon(1+\epsilon)}\sin(2\phi_{T_T}) F_{UT_{TT}}^{\cos(3\phi_h-2\phi_{T_T})} \\ &\quad + T_{TT}(2\lambda_e)\sqrt{2\epsilon(1-\epsilon)}\cos(2\phi_{T_T}) F_{LT_{TT}}^{\sin(3\phi_h-2\phi_{T_T})}. \end{aligned} \tag{5.17b}$$

They contain terms with transverse vector polarization, $S_T$, and with mixed and transverse tensor polarization, $T_{LT}$ and $T_{TT}$. The terms can be separated through their dependence on the polarization angles $\phi_S$ and $\phi_{T_L}, \phi_{T_T}$. For example,

$$\begin{aligned}&\langle \mathcal{F} \rangle_{\cos 3\phi_h}(\phi_S = 0, \phi_{T_L} = \phi_{T_T} = 0) \\ &\quad = T_{LT}\epsilon F_{UT_{LT}}^{\cos(3\phi_h-\phi_{T_L})} \\ &\qquad + T_{TT}\sqrt{2\epsilon(1+\epsilon)}F_{UT_{TT}}^{\cos(3\phi_h-2\phi_{T_T})}, \end{aligned} \tag{5.18a}$$

$$\begin{aligned}&\langle \mathcal{F} \rangle_{\sin 3\phi_h}(\phi_S = \pi/2, \phi_{T_L} = \phi_{T_T} = \pi/2) \\ &\quad = T_{LT}\epsilon F_{UT_{LT}}^{\cos(3\phi_h-\phi_{T_L})} \\ &\qquad - T_{TT}(2\lambda_e)\sqrt{2\epsilon(1-\epsilon)}F_{LT_{TT}}^{\sin(3\phi_h-2\phi_{T_T})}, \end{aligned} \tag{5.18b}$$

which contain only tensor-polarized structures. Such measurements can be performed in pure target spin states polarized relative to the lepton beam axis, in which $\phi_S = \phi_{T_L} = \phi_{T_T} = \phi_N$; see Eq. (5.4). The $n = 4$ averages are

$$\langle \mathcal{F} \rangle_{\cos 4\phi_h} = T_{TT}\epsilon\cos(2\phi_{T_T}) F_{UT_{TT}}^{\cos(4\phi_h-2\phi_{T_T})}, \tag{5.19a}$$

$$\langle \mathcal{F} \rangle_{\sin 4\phi_h} = T_{TT}\epsilon\sin(2\phi_{T_T}) F_{UT_{TT}}^{\cos(4\phi_h-2\phi_{T_T})}, \tag{5.19b}$$

which contain only the transverse tensor-polarized term. The $n = 4$ azimuthal harmonics represent unique features of the spin-1 target and are absent for spin-1/2.

By computing the azimuthal harmonics and choosing appropriate target polarization axes, one can separate vector- and tensor-polarized structures at the cross-section level. Note that in the terms of the cross section where structure functions with $T$ and $L$ photon polarization appear with the same spin and azimuthal angle dependence, the structure functions can only be separated through the dependence on $\epsilon$ (Rosenbluth separation).

The discussion here assumes that the azimuthal harmonics of the cross section are separated by integrating the angular dependence with appropriate weights. In actual experiments the harmonics can also be extracted through fits of the angular dependence, with possibly incomplete angular coverage, and multidimensional fits in several kinematic variables.

### D. Spin asymmetries

Spin asymmetries are ratios of differences and sums of the cross sections in the lepton and target spin variables and are standard observables in the analysis of SIDIS. On the experimental side, the luminosity and detection efficiency cancel in the ratios, reducing the systematic uncertainty. On the theoretical side, the flux factors in the cross section cancel, reducing the kinematic dependence and giving direct access to the structure functions. The theoretical expressions of the asymmetries can generally be represented in the form

$$\begin{aligned}A = \sum &(\text{kinematic factors}) \\ &\times (\text{structure function ratios}), \end{aligned} \tag{5.20}$$

where the kinematic factors (depolarization factors) depend on $\epsilon$ and on the invariant polarization parameters, and the structure function ratios contain the dynamical information on the target structure (depending on the details, these ratios may

have additional kinematic dependencies). With the complex dependence of the spin-1 SIDIS cross section on the target polarization and the final-state hadron momentum, a large variety of asymmetries can be formed and used for experimental analysis. The theoretical expressions can be derived from the formulas of the differential cross section, Eqs. (4.37)–(4.39), and the invariant polarization parameters achieved in measurements with a given pure-state target polarization, Eq. (5.4), et seq. Here we describe only the basic asymmetries of the $\phi_h$-averaged differential cross section for vector and tensor polarization in order to connect with earlier results in Ref. [39] and the experimental literature.

The vector-polarized asymmetry is defined as

$$A^V \equiv \frac{d\sigma(++) - d\sigma(-+) - d\sigma(+-) + d\sigma(--)}{d\sigma(++) + d\sigma(-+) + d\sigma(+-) + d\sigma(--)}, \tag{5.21a}$$

$$d\sigma(\pm\pm) \equiv d\sigma\Big(\lambda_e = \pm\frac{1}{2}, \Lambda = \pm 1\Big). \tag{5.21b}$$

Here the differential cross section is assumed to be averaged over $\phi_h$ [given by Eq. (4.36) with $\mathcal{F} \to \langle\mathcal{F}\rangle_1$, Eq. (5.16)], and differential in the remaining variables of the hadron phase-space element. The differential cross section depends on the lepton helicity $\lambda_e$ and the target spin projection $\Lambda$ along the quantization axis $N$; see Sec. V A. The difference of spin-dependent cross sections in the numerator isolates the vector-polarized structures in the target; the sum in the denominator involves the unpolarized and tensor-polarized structures. The asymmetry takes values $A^V \in [-1, 1]$. The asymmetries for target polarization parallel and perpendicular to the lepton beam are denoted by $\parallel$ and $\perp$ (see Sec. V A). For target polarization parallel to the lepton beam, Eq. (5.5), et seq., the asymmetry becomes

$$A^V_\parallel = D_{\parallel[S_L]} \frac{F_{LS_L}}{\Sigma_\parallel F} + D_{\parallel[S_T]} \frac{F^{\cos\phi_S}_{LS_T}}{\Sigma_\parallel F}, \tag{5.22a}$$

$$\begin{aligned}\Sigma_\parallel F \equiv\ & F_{UU,T} + \epsilon F_{UU,L} \\ & + D_{\parallel[T_{LL}]} \left(F_{UT_{LL},T} + \epsilon F_{UT_{LL},L}\right) \\ & + D_{\parallel[UT_{LT}]} F^{\cos\phi_{T_L}}_{UT_{LT}} + D_{\parallel[T_{TT}]} F^{\cos 2\phi_{T_T}}_{UT_{TT}},\end{aligned} \tag{5.22b}$$

where the kinematic factors $D_{\parallel[S_L]}, \ldots, D_{\parallel[T_{TT}]}$ are given in Ref. [39], Eqs. (3.71) and (3.65). For target polarization perpendicular to the lepton beam, Eq. (5.8a), et seq., the asymmetry becomes

$$A^V_\perp = D_{\perp[S_L]} \frac{F_{LS_L}}{\Sigma_\perp F} + D_{\perp[S_T]} \frac{F^{\cos\phi_S}_{LS_T}}{\Sigma_\perp F}, \tag{5.23a}$$

$$\begin{aligned}\Sigma_\perp F \equiv\ & F_{UU,T} + \epsilon F_{UU,L} \\ & + D_{\perp[T_{LL}]} \left(F_{UT_{LL},T} + \epsilon F_{UT_{LL},L}\right) \\ & + D_{\perp[UT_{LT}]} F^{\cos\phi_{T_L}}_{UT_{LT}} + D_{\perp[T_{TT}]} F^{\cos 2\phi_{T_T}}_{UT_{TT}},\end{aligned} \tag{5.23b}$$

where the kinematic factors $D_{\perp[S_L]}, \ldots, D_{\perp[T_{TT}]}$ are given in Ref. [39], Eqs. (3.72) and (3.66).

The vector-polarized asymmetry Eq. (5.21) is the "two-state asymmetry," where the denominator is formed using only the $\Lambda = \pm 1$ states but not the $\Lambda = 0$ state. (In Ref. [39] this asymmetry is denoted by subscript "(2)," which we drop here for brevity.) One can also consider the three-state asymmetry, where the denominator is the average over all three spin states, $\Lambda = \pm 1$ and 0, and does not involve tensor-polarized structures; the corresponding kinematic factors are given in Ref. [39]. The two-state asymmetry is more interesting because it is easier to measure and is strictly bounded by $[-1, 1]$.

The tensor-polarized asymmetry is defined as

$$A^T \equiv \frac{d\sigma(+) + d\sigma(-) - 2d\sigma(0)}{d\sigma(+) + d\sigma(-) + d\sigma(0)}, \tag{5.24a}$$

$$d\sigma(\Lambda) \equiv \frac{1}{2} \sum_{\lambda_e} d\sigma(\lambda_e, \Lambda). \tag{5.24b}$$

Here the differential cross section is averaged over $\phi_h$. It is averaged over the lepton helicity and depends on the target spin projection $\Lambda$ along the quantization axis $N$; see Sec. V A. The cross-section difference in the numerator isolates the tensor-polarized target structures; the denominator includes only the unpolarized structures. Equation (5.24) takes values $A \in [-2, 1]$. For target polarization parallel to the lepton beam, Eq. (5.5), et seq., the tensor-polarized asymmetry becomes

$$\begin{aligned}A^T_\parallel =\ & 2D_{\parallel[T_{LL}]} \frac{F_{UT_{LL},T} + \epsilon F_{UT_{LL},L}}{F_U} \\ & + 2D_{\parallel[UT_{LT}]} \frac{F^{\cos\phi_{T_L}}_{UT_{LT}}}{F_U} + 2D_{\parallel[T_{TT}]} \frac{F^{\cos 2\phi_{T_T}}_{UT_{TT}}}{F_U},\end{aligned} \tag{5.25a}$$

$$F_U \equiv F_{UU,T} + \epsilon F_{UU,L}. \tag{5.25b}$$

The kinematic factors $D_{\parallel[T_{LL}]}$, $D_{\parallel[UT_{LT}]}$, and $D_{\parallel[T_{TT}]}$ are given in Ref. [39], Eq. (3.65); the same factors appear in the denominator of the vector-polarized asymmetry Eq. (5.22). Likewise, for target polarization perpendicular to the lepton beam, Eq. (5.8a), et seq., the tensor-polarized asymmetry becomes

$$\begin{aligned}A^T_\perp =\ & 2D_{\perp[T_{LL}]} \frac{F_{UT_{LL},T} + \epsilon F_{UT_{LL},L}}{F_U} \\ & + 2D_{\perp[UT_{LT}]} \frac{F^{\cos\phi_{T_L}}_{UT_{LT}}}{F_U} + 2D_{\perp[T_{TT}]} \frac{F^{\cos 2\phi_{T_T}}_{UT_{TT}}}{F_U},\end{aligned} \tag{5.26a}$$

where the denominator $F_U$ is the same as in Eq. (5.25). The kinematic factors $D_{\perp[T_{LL}]}$, $D_{\perp[UT_{LT}]}$, and $D_{\perp[T_{TT}]}$ are given in Ref. [39], Eq. (3.66).

The spin asymmetries considered here are for the $\phi_h$-averaged differential cross section. More complex spin asymmetries can be formed from the $\phi_h$-dependent differential cross section, where all the terms in the differential cross section contribute. The corresponding expressions can be derived from the general decomposition of the cross section Eq. (4.36). In particular, when the $\phi_h$ dependence is included, one can form: (i) lepton single-spin asymmetries, involving the $\lambda_e$ dependent term of $\mathcal{F}_U$; (ii) vector-polarized target single-spin asymmetries, involving the $S_L$ and $S_T$ dependent terms in $\mathcal{F}_S$; (iii) tensor-polarized double-spin asymmetries, involving the $T_{LL}\lambda_e$, $T_{LT}\lambda_e$, and $T_{TT}\lambda_e$ dependent terms in $\mathcal{F}_T$.

## VI. SUMMARY

In this work we have derived the general form of the cross section for SIDIS on a polarized spin-1 target. The expressions obtained are general and do not rely on assumptions about strong interaction dynamics (only $P$ and $T$ invariance). The kinematic factors are presented in their exact form, and the cross-section decomposition can be used at all energies, in the deep-inelastic regime as well as in low-energy hadron production or nuclear breakup processes.

Special attention has been paid to a relativistically covariant formulation of the target polarization and the final-state hadron distributions. The orthonormal basis four-vectors can be constructed from the particle momenta in any reference frame where they are available, and the invariant polarization parameters and final-state variables can be computed as scalar products from the four-vector components in that reference frame. The covariant spin density matrix of the spin-1 target can be specified in any frame where the experimental polarization is available (e.g., the target rest frame). This enables simple and efficient calculations and avoids the use of explicit Lorentz transformations.

At the same time, the covariant expressions can be evaluated and interpreted in the class of collinear frames, where they have a simple interpretation. The class of collinear frames contains the target rest frame as a special instance. The connection with the target rest frame is useful for fixed-target experiments, where target polarization and the kinematic vectors are directly given in the target rest frame; and for colliding-beam experiments, where the polarization of the beam particle has a simple relation to that in the rest frame.

The form of the SIDIS cross section for the vector-polarized spin-1 target is the same as for the polarized spin-1/2 target. The new feature of the spin-1 target is the presence of tensor-polarized structures, which include lepton helicity-independent and dependent structures and give rise to new azimuthal modulations, including unique $\cos(4\phi_h)$ and $\sin(4\phi_h)$ dependencies. Measurement of these azimuthal modulations could demonstrate the presence of nonzero tensor polarization in the target without polarimetry.

The general form of the cross section obtained here can be applied to SIDIS on the polarized deuteron in the current fragmentation region (identified hadron/jets). In the asymptotic regime the SIDIS structure functions can be computed using QCD factorization and become convolutions of TMD parton densities and fragmentation functions [9]. Extensive efforts have been made in analyzing these structures for the spin-1/2 target; the techniques can be extended to the spin-1 target (see Ref. [32]).

The results obtained here can also be applied to SIDIS on the polarized deuteron in the target fragmentation region, in particular the nuclear breakup process (spectator nucleon tagging). For this process the semi-inclusive structure functions can be computed by separating nuclear and nucleon structure and using low-energy nuclear dynamics to predict the nuclear momentum distributions and breakup amplitudes; see Part II [1]. Large tensor polarization effects can be achieved by selecting final states with spectator momenta ≈300–400 MeV (in the deuteron rest frame), where the $D$-wave in the deuteron wave function is dominant.

The structural analysis of the semi-inclusive cross section presented here can be extended from the spin-1 target to higher-spin targets. The basic steps are outlined in Appendix D.

The present study describes tensor-polarized structures in the cross section of scattering on a spin-1 target, supported by the polarization of the initial state. Tensor-polarized structures can also appear in hadronic processes with spin-1/2 → spin-3/2 transitions, when formed from the spin variables in the initial and final states. For example, a tensor-polarized parton density appears in the $N \to \Delta$ transition and can be studied in the context of generalized parton distributions [64]. Tensor-polarized observables using final-state spin variables could also be formed in SIDIS. One example would be SIDIS on the polarized nucleon with detection of a $\Delta$ in the target fragmentation region, in which the $\Delta \to \pi N$ decay distribution is coupled with the spin of the $\Delta$. This process can be analyzed using QCD factorization with fracture functions and deserves further study [34,36].

## ACKNOWLEDGMENTS

This study greatly benefited from discussions with A. Bacchetta, S. Kumano, and F. Vera. This material is based upon work supported by the U.S. Department of Energy, Office of Science, Office of Nuclear Physics, under Contract No. DE-AC05-06OR23177 and by the U.S. National Science Foundation under Awards No. PHY-2111442 and No. PHY-2239274.

## DATA AVAILABILITY

There are no publicly available research data or software supporting this manuscript. Requests for further information or data should be sent to the authors.

## APPENDIX A: CORRESPONDENCE WITH EARLIER WORK

In this appendix we summarize the changes in definitions relative to our earlier work [39]. The changes are caused by our use of the Trento convention for the azimuthal angles in the present work.

(i) Azimuthal hadron and target spin angles

$$\phi_h \text{ (present)} = -\phi_p \text{ (Ref. [39])}, \tag{A1}$$

$$\phi_s \text{ (present)} = -\phi_s \text{ (Ref. [39])}. \tag{A2}$$

(ii) Angle of target polarization transverse to lepton beam ($\perp$ polarization)

$$\psi_N \text{ (present)} = -\phi_N \text{ (Ref. [39])}. \tag{A3}$$

In the present work we denote the polarization angle around the lepton beam axis by $\psi_N$, to distinguish it from the collinear-frame angles around the photon axis. We measure the polarization angle in the same sense as the collinear frame angles in the Trento convention.

(iii) Transverse basis vectors

$$e_x \text{ (present)} = e_{T1} \text{ (Ref. [39])}, \tag{A4}$$

$$e_y \text{ (present)} = e_{T2} \text{ (Ref. [39])}. \tag{A5}$$

## APPENDIX B: DENSITY MATRIX FROM SPIN OPERATOR

In this appendix we present an alternative derivation of the form of the spin density matrix of the moving spin-1 system, using the language of quantum-mechanical states and operators. It starts from the three-dimensional form of the density matrix in the rest frame and constructs its four-dimensional generalization.

The density matrix $\rho$ of a spin-1 system is a $3 \times 3$ Hermitean matrix with unit trace, $\mathrm{Tr}[\rho] = 1$. In the rest frame of the spin-1 system, it can be specified in a basis of single-particle states $|\boldsymbol{P} = \boldsymbol{0}; \lambda\rangle$, where the momentum is zero and the spin is quantized along the $z$ axis, with spin projection $\lambda = (+1, 0, -1)$. The density matrix can be parametrized in the form [65]

$$\begin{aligned}\rho &\equiv \rho(\lambda, \lambda') \\ &= \tfrac{1}{3} + \tfrac{1}{2} S^i \mathscr{S}^i + \tfrac{1}{2} T^{ij} \big( \mathscr{S}^i \mathscr{S}^j + \mathscr{S}^j \mathscr{S}^i - \tfrac{4}{3} \delta^{ij} \big),\end{aligned} \tag{B1}$$

where $\mathscr{S}^{i(j)}$ are the $3 \times 3$ matrices describing the spin operators in the spin-1 representation. In the $|\boldsymbol{P} = \boldsymbol{0}; \lambda\rangle$ basis quantized along the $z$ axis, these take the form

$$\mathscr{S}^x = \frac{1}{\sqrt{2}} \begin{pmatrix} 0 & 1 & 0 \\ 1 & 0 & 1 \\ 0 & 1 & 0 \end{pmatrix}, \tag{B2a}$$

$$\mathscr{S}^y = \frac{i}{\sqrt{2}} \begin{pmatrix} 0 & -1 & 0 \\ 1 & 0 & -1 \\ 0 & 1 & 0 \end{pmatrix}, \tag{B2b}$$

$$\mathscr{S}^z = \begin{pmatrix} 1 & 0 & 0 \\ 0 & 0 & 0 \\ 0 & 0 & -1 \end{pmatrix}, \tag{B2c}$$

and $i, j = (x, y, z)$ denote the Cartesian components. The parameters in Eq. (B1) are a three-dimensional pseudovector $S^i$ and a traceless symmetric tensor $T^{ij}$. They coincide, respectively, with the expectation value of the spin operators and their traceless tensor product

$$S^i = \mathrm{Tr}[\rho \mathscr{S}^i] = \langle \mathscr{S}^i \rangle, \tag{B3a}$$

$$\begin{aligned} T^{ij} &= \tfrac{1}{2} \mathrm{Tr}\big[\rho \big( \mathscr{S}^i \mathscr{S}^j + \mathscr{S}^j \mathscr{S}^i - \tfrac{4}{3} \delta^{ij} \big)\big] \\ &= \tfrac{1}{2} \big( \langle \mathscr{S}^i \mathscr{S}^j + \mathscr{S}^j \mathscr{S}^i \rangle - \tfrac{4}{3} \delta^{ij} \big). \end{aligned} \tag{B3b}$$

In this way the spin-1 density matrix is completely specified by a set of expectation values that can be determined experimentally through spin measurements along certain directions.[4] Under an active three-rotation $R$ of the rest frame spin-1 system, the parameters $S^i$ and $T^{ij}$ transform as

$$S'^i = R^{ij} S^j, \quad T'^{ij} = R^{ik} T^{kl} (R^{-1})^{lj}. \tag{B4}$$

In the rest frame, we can make any choice of axes used in Eq. (B1). In what follows for the application to the semi-inclusive scattering process, we make the choice corresponding to the $(x'y'z)$-system in Fig. 1. This is the natural choice, having the $z$ axis aligned with the collinear axis. A straightforward longitudinal boost links the target rest frame and any general collinear frame, and the separation in longitudinal/transverse spin corresponds to $z$, respectively transverse components of the spin vector $\boldsymbol{S}$ and tensor $T$, see Sec. III.B.

The parametrization Eq. (B1) can be extended to a moving spin-1 system by replacing the zero–momentum single-particle states by states with momentum $\boldsymbol{P} \neq 0$, defined by the action of a standard Lorentz boost $L(P/M)$ acting on the rest frame states $|\boldsymbol{P} = \boldsymbol{0}; \lambda\rangle$,

$$|P, \lambda\rangle \equiv U[L(P/M)]\ |(M, \boldsymbol{0}), \lambda\rangle. \tag{B5}$$

Here the form of $L(P^\mu/M)$ depends on the choice of dynamics and spin, e.g., canonical, helicity, or light-front helicity [66].

Under a general Lorentz transformation $\Lambda$, the spin variables of the states Eq. (B5) transform through a Wigner rotation (little group transformation), which depends on the transformation $\Lambda$, the particle momentum $P$, and the choice of the standard Lorentz boost $L$ used in defining the states:

$$U(\Lambda)|P, \lambda\rangle = \sum_{\lambda'} |\Lambda P, \lambda'\rangle\, R_w(\Lambda, P/M)_{\lambda'\lambda}, \tag{B6}$$

where the Wigner rotation takes the form

$$R_w(\Lambda, P/M) \equiv L^{-1}[(\Lambda P)/M]\ \Lambda\ L(P/M). \tag{B7}$$

The Wigner rotation affects also the density matrix $\rho(\lambda, \lambda')$. The rotation of the spin variables can be expressed as a three-dimensional spatial rotation of the parameters $S^i$ and $T^{ij}$, of the same form as Eq. (B4), but with the rotation matrix $R$ given by the Wigner rotation matrix Eq. (B7). This leads to a change in the density matrix after a general Lorentz transformation, where due to the Wigner rotation the values of the matrix elements depend both on the choice of type of spin and the momentum of the particle. If the density matrix parameters are determined through intensity measurements in the ensemble rest frame, then the parameters in any frame where the particle is moving can be obtained by applying Eq. (B4) using the relevant Wigner rotation. The covariant density matrix of Eq. (3.4) avoids these complications as the Wigner rotations cancel between $\rho(\lambda, \lambda')$ and the particle wave functions $\epsilon^\mu(\lambda)$. Overall, the covariant density matrix transforms covariantly, independent of ensemble momentum or type of spin that is considered.

If one boosts from a reference rest frame to a moving frame using the standard boosts, then Eq. (B7) shows $R_w(\Lambda, P/M) = 1$, and the density matrix in the moving frame is identical to that of the rest frame. Between different forms of dynamics, however, different standard boosts do not result in the same moving frame. The timelike direction of the reference rest frame will have been boosted to the same four-vector $e_P$, but the spatial directions corresponding to the boosted $xyz$ axes will be different for different choices of spin. This difference is encoded in an additional rest frame rotation, usually referred to as the Melosh rotation. If we want to compare density matrices in the *same* moving frame between different

[4] This formulation is analogous to the parametrization of the photon polarization density matrix through Stokes parameters [60].

spinor types, then we have to include this additional rest frame rotation in the transformations from the reference rest frame before carrying out the standard boosts. This changes the density matrix as in Eq. (B4) and yields different density matrices for different choices of spin in the *same* moving frame (but also different polarization wave functions).

In Sec. III D, the complications related to Wigner rotations are avoided by the choice made in Eqs. (3.27) to write the polarization basis for the spin-1 target using the coordinate independent basis. This choice fixes the density matrix for the class of collinear frames (including a target rest frame) to that of Eq. (3.28). These frames are linked to each other by collinear boosts, which only involve trivial Wigner rotations (= 1) for the density matrix. This does not prohibit the use of a frame where the target has transverse momentum. The calculations of the elements in Eq. (3.28) only involve invariants, which can be computed in any frame. Its physical interpretation, however, is tied to the class of collinear frames and happens in coordinate independent fashion through the basis construction.

Using the moving states of Eq. (B5), one can introduce a spin four-vector and a symmetric traceless spin four-tensor, which generalize the three-dimensional quantities in the rest frame, Eqs. (B3a) and (B3b). They are defined as the expectation values

$$S^\mu = \langle \hat{W}^\mu \rangle, \tag{B8a}$$

$$T^{\mu\nu} = \frac{1}{3}\left\langle \hat{W}^\mu \hat{W}^\nu + \hat{W}^\nu \hat{W}^\mu + \frac{4}{3}\left( g^{\mu\nu} - \frac{\hat{P}^\mu \hat{P}^\nu}{M^2} \right) \right\rangle, \tag{B8b}$$

where $\hat{W}^\mu$ is the Pauli-Lubanski operator

$$\hat{W}^\mu = \frac{1}{2M}\epsilon^{\mu\nu\rho\sigma}\hat{M}_{\nu\rho}\hat{P}_\sigma, \tag{B9}$$

with $\hat{P}^\mu$ and $\hat{M}^{\nu\rho}$ the generators of space-time translations and proper Lorentz transformations as defined in Ref. [65]. It can be shown that the $S^\mu$ and $T^{\mu\nu}$ defined as such correspond to the parameters used in the covariant density matrix introduced earlier in Eq. (3.4).

## APPENDIX C: STRUCTURE FUNCTIONS AS HELICITY AMPLITUDES

In this appendix we present an alternative derivation of the independent structures in the spin-1 semi-inclusive cross section using projections of the hadronic tensor on target and virtual photon helicity states. The projections can be viewed as physical cross sections of the $\gamma^* + A \to h + X$ process with definite helicities of the initial particles (with diagonal and interference terms). The 41 structure functions introduced in Sec. IV B can be expressed as linear combinations of the helicity projections.

The target and virtual photon helicity states are defined in a collinear frame using the $x'y'z$ coordinate system. The spin wave functions can be expressed covariantly in terms of the longitudinal basis vectors of set II, Eq. (2.7), and the transverse basis vectors aligned with the final hadron momentum, Eq. (2.15). For the target helicity states the wave functions are given by Eq. (3.27) and are the same as those in the spin density matrix Eq. (3.28). For the virtual photon, because the three-momentum is in the negative $z$ direction, the wave functions are constructed with the $y'$ and $z$ axis flipped [65], which leads to

$$\epsilon^\mu(\kappa = 0) = e_L^\mu, \tag{C1a}$$

$$\epsilon^\mu(\kappa = \pm 1) = \mp\frac{1}{\sqrt{2}}\left(e_{x'}^\mu \mp i e_{y'}^\mu\right). \tag{C1b}$$

The helicity projections of the hadronic tensor are then defined as

$$F_{\kappa'\kappa}^{\lambda'\lambda} \equiv \epsilon^{\mu *}(\kappa') W_{\mu\nu}(\lambda', \lambda)\epsilon^\nu(\kappa), \tag{C2}$$

where $W_{\mu\nu}(\lambda', \lambda)$ is given in Eq. (4.7) and corresponds to the target helicity states Eq. (3.27). The helicity projections obey the following conditions due to Hermiticity and parity invariance:

$$F_{\kappa'\kappa}^{\lambda'\lambda} = \left(F_{\kappa\kappa'}^{\lambda\lambda'}\right)^*, \tag{C3a}$$

$$F_{-\kappa'-\kappa}^{-\lambda'-\lambda} = (-1)^{\lambda-\lambda'+\kappa-\kappa'} F_{\kappa'\kappa}^{\lambda'\lambda}. \tag{C3b}$$

The conditions reduce the number of independent helicity projections. Imposing the Hermiticity condition we have $3^4 = 81$ independent real amplitudes; imposing also the parity invariance condition we are left with 41 (there is no constraint on the $F_{00}^{00}$ amplitude). Thus the number of independent real helicity projections is equal to the total number of structure functions determined by the enumeration of independent structures in Sec. IV B.

The structure functions of Sec. IV B can be expressed as linear combinations of the helicity projections of the hadronic tensor, by contracting the independent tensor structures of Eqs. (4.20)–(4.31) with the virtual photon helicity wave functions Eq. (C1). We obtain for the structure functions with unpolarized target

$$F_{UU,L} = \frac{2}{3}\left(2F_{00}^{++} + F_{00}^{00}\right), \tag{C4a}$$

$$F_{UU,T} = \frac{2}{3}(F_{++}^{++} + F_{++}^{00} + F_{++}^{--}), \tag{C4b}$$

$$F_{UU}^{\cos\phi_h} = -\frac{2\sqrt{2}}{3}\,\mathrm{Re}\left(F_{+0}^{++} + F_{+0}^{00} + F_{+0}^{--}\right), \tag{C4c}$$

$$F_{UU}^{\cos 2\phi_h} = -\frac{2}{3}\,\mathrm{Re}(2F_{+-}^{++} + F_{+-}^{00}), \tag{C4d}$$

$$F_{LU}^{\sin\phi_h} = -\frac{2\sqrt{2}}{3}\,\mathrm{Im}\left(F_{+0}^{++} + F_{+0}^{00} + F_{+0}^{--}\right); \tag{C4e}$$

for the structure functions with longitudinal vector target polarization

$$F_{US_L}^{\sin\phi_h} = -\sqrt{2}\,\mathrm{Im}(F_{+0}^{++} - F_{+0}^{--}), \tag{C5a}$$

$$F_{US_L}^{\sin 2\phi_h} = -2\,\mathrm{Im}\,F_{+-}^{++}, \tag{C5b}$$

$$F_{LS_L} = F_{++}^{++} - F_{++}^{--}, \tag{C5c}$$

$$F_{LS_L}^{\cos\phi_h} = -\sqrt{2}\,\mathrm{Re}(F_{+0}^{++} - F_{+0}^{--}); \tag{C5d}$$

for the structure functions with transverse vector target polarization

$$F_{US_T,L}^{\sin(\phi_h-\phi_S)} = -2\sqrt{2}\,\mathrm{Im}\,F_{00}^{+0}, \tag{C6a}$$
$$F_{US_T,T}^{\sin(\phi_h-\phi_S)} = -\sqrt{2}\,\mathrm{Re}(F_{++}^{+0} - F_{++}^{-0}), \tag{C6b}$$
$$F_{US_T}^{\sin(\phi_h+\phi_S)} = -\sqrt{2}\,\mathrm{Im}\,F_{+-}^{+0}, \tag{C6c}$$
$$F_{US_T}^{\sin(3\phi_h-\phi_S)} = -\sqrt{2}\,\mathrm{Im}\,F_{+-}^{-0}, \tag{C6d}$$
$$F_{US_T}^{\sin\phi_S} = -\,\mathrm{Im}\,\big(F_{+0}^{+0} + F_{+0}^{0-}\big), \tag{C6e}$$
$$F_{US_T}^{\sin(2\phi_h-\phi_S)} = -\,\mathrm{Im}\,\big(F_{+0}^{0+} - F_{+0}^{-0}\big), \tag{C6f}$$
$$F_{LS_T}^{\cos(\phi_h+\phi_S)} = \sqrt{2}\,\mathrm{Re}(F_{++}^{+0} + F_{++}^{-0}), \tag{C6g}$$
$$F_{LS_T}^{\cos\phi_S} = -\,\mathrm{Re}\,\big(F_{+0}^{+0} + F_{+0}^{0-}\big), \tag{C6h}$$
$$F_{LS_T}^{\cos(2\phi_h-\phi_S)} = -\,\mathrm{Re}\,\big(F_{+0}^{0+} + F_{+0}^{-0}\big); \tag{C6i}$$

for the structure functions with purely longitudinal tensor target polarization

$$F_{UT_{LL},L} = 2\big(F_{00}^{++} - F_{00}^{00}\big), \tag{C7a}$$
$$F_{UT_{LL},T} = (F_{++}^{++} - 2F_{++}^{00} + F_{++}^{--}), \tag{C7b}$$
$$F_{UT_{LL}}^{\cos\phi_h} = -\sqrt{2}\,\mathrm{Re}\,\big(F_{+0}^{++} - 2F_{+0}^{00} + F_{+0}^{--}\big), \tag{C7c}$$
$$F_{UT_{LL}}^{\cos 2\phi_h} = -2\,\mathrm{Re}(F_{+-}^{++} - F_{+-}^{00}), \tag{C7d}$$
$$F_{LT_{LL}}^{\sin\phi_h} = -\sqrt{2}\,\mathrm{Im}\,\big(F_{+0}^{++} - 2F_{+0}^{00} + F_{+0}^{--}\big); \tag{C7e}$$

for the structure functions with longitudinal-transverse tensor target polarization

$$F_{UT_{LT},L}^{\cos(\phi_h-\phi_{T_L})} = 4\sqrt{2}\,\mathrm{Re}\,F_{00}^{+0}, \tag{C8a}$$
$$F_{UT_{LT},T}^{\cos(\phi_h-\phi_{T_L})} = 2\sqrt{2}\,\mathrm{Re}(F_{++}^{+0} - F_{++}^{-0}), \tag{C8b}$$
$$F_{UT_{LT}}^{\cos(\phi_h+\phi_{T_L})} = -2\sqrt{2}\,\mathrm{Re}\,F_{+-}^{+0}, \tag{C8c}$$
$$F_{UT_{LT}}^{\cos(3\phi_h-\phi_{T_L})} = 2\sqrt{2}\,\mathrm{Re}\,F_{+-}^{-0}, \tag{C8d}$$
$$F_{UT_{LT}}^{\cos\phi_{T_L}} = -2\,\mathrm{Re}\,\big(F_{+0}^{+0} - F_{+0}^{0-}\big), \tag{C8e}$$
$$F_{UT_{LT}}^{\cos(2\phi_h-\phi_{T_L})} = -2\,\mathrm{Re}\,\big(F_{+0}^{0+} - F_{+0}^{-0}\big), \tag{C8f}$$
$$F_{LT_{LT}}^{\sin(\phi_h+\phi_{T_L})} = -2\sqrt{2}\,\mathrm{Im}(F_{++}^{+0} + F_{++}^{-0}), \tag{C8g}$$
$$F_{LT_{LT}}^{\sin\phi_{T_L}} = -2\,\mathrm{Im}\,\big(F_{+0}^{+0} - F_{+0}^{0-}\big), \tag{C8h}$$
$$F_{LT_{LT}}^{\sin(2\phi_h-\phi_{T_L})} = -2\,\mathrm{Im}\,\big(F_{+0}^{0+} - F_{+0}^{-0}\big); \tag{C8i}$$

and for the structure functions with purely transverse tensor target polarization

$$F_{UT_{TT},L}^{\cos(2\phi_h-2\phi_{T_T})} = 2\,\mathrm{Re}\,F_{00}^{+-}, \tag{C9a}$$
$$F_{UT_{TT},T}^{\cos(2\phi_h-2\phi_{T_T})} = 2\,\mathrm{Re}\,F_{++}^{+-}, \tag{C9b}$$
$$F_{UT_{TT}}^{\cos 2\phi_{T_T}} = -\,\mathrm{Re}\,F_{+-}^{+-}, \tag{C9c}$$
$$F_{UT_{TT}}^{\cos(4\phi_h-2\phi_{T_T})} = -\,\mathrm{Re}\,F_{+-}^{-+}, \tag{C9d}$$
$$F_{UT_{TT}}^{\cos(\phi_h-2\phi_{T_T})} = -\sqrt{2}\,\mathrm{Re}\,F_{+0}^{+-}, \tag{C9e}$$
$$F_{UT_{TT}}^{\cos(3\phi_h-2\phi_{T_T})} = -\sqrt{2}\,\mathrm{Re}\,F_{+0}^{-+}, \tag{C9f}$$
$$F_{LT_{TT}}^{\sin(2\phi_h-2\phi_{T_T})} = -2\,\mathrm{Im}\,F_{++}^{+-}, \tag{C9g}$$
$$F_{LT_{TT}}^{\sin(\phi_h-2\phi_{T_T})} = \mathrm{Im}\,F_{+0}^{+-}, \tag{C9h}$$
$$F_{LT_{TT}}^{\sin(3\phi_h-2\phi_{T_T})} = -\,\mathrm{Im}\,F_{+0}^{-+}. \tag{C9i}$$

One observes that in each structure function the integer factor before $\phi_h$ is equal to the difference of the total helicities of the $\gamma^*A$ system on the left $(\kappa - \lambda)$ and right side $(\kappa' - \lambda')$ of the projection (the "initial" and "final" state if it were the amplitude of a scattering process),

$$m\phi_h, \quad |m| = |(\kappa - \lambda) - (\kappa' - \lambda')|. \tag{C10}$$

This expresses the conservation of the angular momentum projection on the $z$ axis.

## APPENDIX D: EXTENSION TO HIGHER-SPIN TARGETS

In this appendix we outline the extension of the structural decomposition of the semi-inclusive cross section to targets of spin $>1$. While there are no current plans for polarized measurements on targets of higher spin, there are many atomic nuclei and hadrons with spin $>1$ [67]. From a theoretical viewpoint, the multipole structure of hadronic matrix elements of QCD operators is also of general interest [68,69]. The structure of the polarization parameters, structure functions, and azimuthal dependencies follows a pattern that can be iterated. A density matrix representing a spin-$j$ ensemble can be decomposed into $l = 0, \ldots, 2j$ multipoles of the rotation group. Compared to the preceding spin $j - 1/2$ case, a spin-$j$ target introduces a new $l = 2j$ multipole in the target density matrix with $2(2j) + 1$ polarization parameters $(m_l = -l, \ldots, l)$. These parameters can be collected in a symmetric and traceless rank-$2j$ regular tensor for whole-valued $j$ and pseudotensor for half-valued $j$. For the covariant density matrix, these multipole tensors are Lorentz tensors denoted as $P^{\mu_1\cdots\mu_{2j}}$ here; see the discussion for spin-1 in Sec. III A. The tensors are orthogonal to the target four-momentum in all their indices.

The polarization parameters that appear in the cross-section decomposition can be written as invariant projections of this tensor on the $L, T$ subspaces relative to the hadronic scattering plane and collinear axis, see Eq. (3.12) for the spin-1 case. New terms in the decomposition of the hadronic tensor emerge by combining these invariant polarization parameters with the independent tensors $\mathcal{A}_i^{\mu\nu}$ and a scalar structure function. Only terms that transform as regular tensors are formed; see Sec. IV B. The kinematic dependence of the new terms on $\epsilon$ is determined by the $\mathcal{A}_i^{\mu\nu}$ that appear in each new term, and their contraction with the leptonic tensor; see Eqs. (4.35). The following general pattern emerges, which already became apparent for the spin-1 case:

(1) The azimuthal dependence alternates between sin and cos and reflects the parity of the terms. This follows the pattern
   (a) cos dependence for even parity: $l$ = even multipole combined with unpolarized lepton or $l$ = odd multipole combined with polarized lepton.

(b) sin dependence for odd parity: $l =$ odd multipole combined with unpolarized lepton or $l =$ even multipole combined with polarized lepton.

(2) The polarization parameter

$$P_{L\cdots L} = e^{\mu_1}_{L*} \cdots e^{\mu_{2j}}_{L*} P_{\mu_1\cdots\mu_{2j}}, \tag{D1}$$

which is the projection on the $L$ subspace in all indices, generates five (whole-valued $j$) or four (half-valued $j$) new structure functions. This is the $m_l = 0$ part of the new multipole in the density matrix. The azimuthal dependence of the structure functions is identical to those of the unpolarized target (five structure functions) or $S_L$ (four) case and only involves multiples of $\phi_h$ without any offset angles related to polarization.

(3) Each projection $P_{L\cdots LT}, P_{L\cdots LTT}, \ldots$ on a mixed $L, T$ subspace results in nine new structure functions. These are the $0 < |m_l| < l$ harmonics, where $|m_l|$ corresponds to the number of indices that are projected on the $T$ subspace. The azimuthal and $\epsilon$ dependence follows that from lower spin multipoles with the same $m_l$ value (same $n\phi_h$ dependence, offset angle multiplied with $|m_l|$), albeit with a different offset angle characterizing the higher $l = 2j$ multipole and a change between cos / sin dependence if the parity has changed. Compare the $S_T$ and $T_{LT}$ parts in Eqs. (4.38) and (4.39) for an illustration of this pattern in the spin-1 case.

(4) $P_{T\cdots T}$, the projection of the polarization tensor on the $T$ subspace in all indices, generates nine new structure functions. This is the $m_l = \pm l$ multipole. The structure functions carry azimuthal dependencies with one more unit of $\phi_h$ compared to the $m_l = l - 1 = 2j - 1$ structure functions, including a new $(2j + 2)\phi_h$ modulation, and with a new $l\phi_{T\cdots T}$ offset angle. The new terms have a similar dependence on $\epsilon$ as the preceding $m_l = 1, \ldots, l - 1$ multipoles.

(5) In total the SIDIS cross section for a spin-$j$ target has

$$5 + (2j \times 9) \quad \text{(whole-valued } j\text{)}$$
$$4 + (2j \times 9) \quad \text{(half-valued } j\text{)}$$

new structure functions compared to the previous spin case. This leads to the following series for the lowest spin cases:

$$5, 18, 41, 72, 113, \ldots.$$

These values can be compared to the counting based on helicity projections of the hadronic tensor, which follows (see Appendix C)

$$\left\lceil \frac{3^2}{2} \times (2j+1)^2 \right\rceil, \tag{D2}$$

where we used the ceiling function to round to the next integer for whole-valued $j$. This is related to parity not providing a constraint on the $F^{00}_{00}$ helicity projection in those cases. One can check that this equation generates the same series.

## APPENDIX E: CORRESPONDENCE WITH ZBKLZ

In this appendix we explain the correspondence of our semi-inclusive cross section parametrization with that of Ref. [32] (ZBKLZ), where spin-1 SIDIS in the current fragmentation region is studied in the context of TMD factorization.

The spin-1 semi-inclusive cross section parametrization obtained in our work is general: It is based on general principles (relativistic invariance, discrete symmetries), valid in all kinematic regions (current and target fragmentation regions, finite $Q^2$ and $W$), and makes no assumptions about dynamics. In Ref. [32] the spin-1 semi-inclusive cross section is studied in SIDIS kinematics in the current fragmentation region, where it can be computed using the TMD factorization approximation [9], extending earlier results for the spin-1/2 target [53–55]. The results of that work can be expressed in terms of our general structure functions.

In Ref. [32] the longitudinal hadron momentum is described by the energy fraction variable $z_h$, Eq. (2.25), which takes values $z_h = \mathcal{O}(1)$ in the current fragmentation region. It is related to our light-front minus momentum fraction variable $\eta_h$, Eq. (2.32b), by

$$z_h = \eta_h \left[ 1 + x_A(1 + x_A)\frac{M^2}{Q^2} \right] + \mathcal{O}\left( \frac{M^4}{Q^4}, \frac{M^2 M_h^2}{Q^4} \right); \tag{E1}$$

the dependence on the hadron mass $M_h$ and nonlinear terms $\sim 1/\eta_h$ in the relation enter only at the level of $1/Q^4$ power corrections. The invariant phase-space element Eq. (2.40) is thus expressed in the $z_h$ variable as

$$d\Gamma_{P_h} = \frac{1}{2(2\pi)^3} \frac{dz_h}{z_h} d^2 P_{hT}; \tag{E2}$$

the expression is valid up to $1/Q^4$ power corrections.

In Ref. [32] the differential cross section is presented as [we arrange the expression in a form that can be compared directly with our Eq. (4.36)]

$$d\sigma = \frac{2\pi\alpha_{\rm em}^2 y^2}{Q^2(1-\epsilon)} dx_A \frac{dy}{y} \frac{d\psi_{l'}}{2\pi} \times \frac{I}{x_A}(\mathcal{F}'_U + \mathcal{F}'_S + \mathcal{F}'_T)\, dz_h \frac{d|\boldsymbol{P}_{hT}|^2}{2} d\phi_h. \tag{E3}$$

The factor in the first line depends on the electron variables and is identical to the one in Eq. (4.36); because of Eq. (2.5),

$$\frac{dy}{y} = \frac{dQ^2}{Q^2} \quad (x_A \text{ fixed}). \tag{E4}$$

The factor

$$I \equiv 1 + \frac{\gamma^2}{2x_A} = 1 + \mathcal{O}\left(\frac{M^2}{Q^2}\right) \tag{E5}$$

in the second line of Eq. (E3) arises from the relation between the semi-inclusive and inclusive structure functions quoted in Ref. [53] and influences the normalization of the semi-inclusive structure functions; $I = 1$ in the DIS limit. The combination

$$\frac{d|\boldsymbol{P}_{hT}|^2}{2} d\phi_h = d^2 P_{hT} \tag{E6}$$

in Eq. (E3) represents the transverse phase-space element. The functions $\mathcal{F}'_U$, $\mathcal{F}'_S$, $\mathcal{F}'_T$ in Eq. (E3) contain the target spin and $\phi_h$-dependent structures and are given in Ref. [32]. The correspondence between the structure functions can be established by comparing the individual structures in Eq. (4.36) and Eq. (E3). Our invariant tensor polarization parameters $T_{LL}$, $T_{LT}$, and $T_{TT}$, Eq. (3.12), are related to the parameters $S_{LL}$, $S_{LT}$, and $S_{TT}$ of Ref. [29] by

$$T_{LL} = \tfrac{2}{3} S_{LL}, \quad T_{LT} = \tfrac{1}{2} S_{LT}, \quad T_{TT} = S_{TT}; \tag{E7}$$

the angles and vector polarization parameters are defined in the same way in both works. The correspondence of the structure functions of the $\phi_h$ independent terms in the cross section (nonzero when averaged over $\phi_h$) is obtained as (ours on the left, Ref. [32] on the right)

$$\begin{Bmatrix} F_{UU,T} \\ F_{UU,L} \\ F_{LS_L} \\ F_{LS_T}^{\cos\phi_S} \\ F_{UT_{LL},T} \\ F_{UT_{LL},L} \\ F_{UT_{LT}}^{\cos\phi_{T_L}} \\ F_{UT_{TT}}^{\cos 2\phi_{T_T}} \end{Bmatrix} = 2(2\pi)^3 \frac{I z_h}{x_A} \begin{Bmatrix} F_{UU,T} \\ F_{UU,L} \\ F_{LL} \\ F_{LT}^{\cos\phi_S} \\ \frac{3}{2} F_{U(LL),T} \\ \frac{3}{2} F_{U(LL),L} \\ 2F_{U(LT)}^{\cos\phi_{LT}} \\ F_{U(TT)}^{\cos(2\phi_{TT})} \end{Bmatrix}. \tag{E8}$$

The correspondence of the structure functions of the $\phi_h$ modulations of the cross section (vanishing when averaged over $\phi_h$) can be obtained in the same way, with identical factors arising in the tensor-polarized structures.


[1] W. Cosyn and C. Weiss, following paper, Semi-inclusive deep-inelastic scattering on a polarized spin-1 target. II. Deuteron and spectator nucleon tagging, Phys. Rev. C **114**, 025202 (2026).

[2] B. Lampe and E. Reya, Spin physics and polarized structure functions, Phys. Rep. **332**, 1 (2000).

[3] S. E. Kuhn, J. P. Chen, and E. Leader, Spin structure of the nucleon—Status and recent results, Prog. Part. Nucl. Phys. **63**, 1 (2009).

[4] C. A. Aidala, S. D. Bass, D. Hasch, and G. K. Mallot, The spin structure of the nucleon, Rev. Mod. Phys. **85**, 655 (2013).

[5] A. Deur, S. J. Brodsky, and G. F. De Téramond, The spin structure of the nucleon, Rep. Prog. Phys. **82**, 076201 (2019).

[6] J. C. Collins, D. E. Soper, and G. F. Sterman, Factorization of hard processes in QCD, Adv. Ser. Direct. High Energy Phys. **5**, 1 (1989).

[7] J. Kodaira and K. Tanaka, Polarized structure functions in QCD, Prog. Theor. Phys. **101**, 191 (1999).

[8] J. Collins, *Foundations of Perturbative QCD* (Cambridge University Press, Cambridge, UK, 2011), Vol. 32.

[9] R. Boussarie *et al.*, TMD handbook, arXiv:2304.03302.

[10] B. Adeva *et al.* (Spin Muon), Polarized quark distributions in the nucleon from semi-inclusive spin asymmetries, Phys. Lett. B **420**, 180 (1998).

[11] A. Airapetian *et al.* (HERMES), Quark helicity distributions in the nucleon for up, down, and strange quarks from semi-inclusive deep-inelastic scattering, Phys. Rev. D **71**, 012003 (2005).

[12] M. Alekseev *et al.* (COMPASS), Flavour separation of helicity distributions from deep inelastic muon-deuteron scattering, Phys. Lett. B **680**, 217 (2009).

[13] M. Alekseev Jr. *et al.* (COMPASS), Collins and Sivers asymmetries for pions and kaons in muon-deuteron DIS, Phys. Lett. B **673**, 127 (2009).

[14] G. D. Alexeev *et al.* (COMPASS), High-statistics measurement of Collins and Sivers asymmetries for transversely polarized deuterons, Phys. Rev. Lett. **133**, 101903 (2024).

[15] L. L. Frankfurt and M. I. Strikman, High momentum transfer processes with polarized deuterons, Nucl. Phys. A **405**, 557 (1983).

[16] P. Hoodbhoy, R. Jaffe, and A. Manohar, Novel effects in deep inelastic scattering from spin-one hadrons, Nucl. Phys. B **312**, 571 (1989).

[17] A. Airapetian *et al.* (HERMES), First measurement of the tensor structure function $b_1$ of the deuteron, Phys. Rev. Lett. **95**, 242001 (2005).

[18] E. Long, Potential for a tensor asymmetry $A_{zz}$ measurement in the $x > 1$ region at Jefferson Lab, J. Phys.: Conf. Ser. **543**, 012010 (2014).

[19] K. Slifer and E. Long, Novel physics with tensor polarized deuteron targets, PoS **PSTP2013**, 008 (2013).

[20] W. Cosyn, B. R. Tomei, A. Sosa, and A. Zec, Polarization options in inclusive DIS off tensor polarized deuteron, Eur. Phys. J. A **61**, 83 (2025).

[21] J. Poudel, A. Bacchetta, J.-P. Chen, and N. Santiesteban, Experimental study of tensor structure function of deuteron, Eur. Phys. J. A **61**, 81 (2025).

[22] H. Khan and P. Hoodbhoy, Convenient parametrization for deep inelastic structure functions of the deuteron, Phys. Rev. C **44**, 1219 (1991).

[23] W. Cosyn, Y.-B. Dong, S. Kumano, and M. Sargsian, Tensor-polarized structure function $b_1$ in the standard convolution description of the deuteron, Phys. Rev. D **95**, 074036 (2017).

[24] G. A. Miller, Pionic and hidden-color, six-quark contributions to the deuteron $b_1$ structure function, Phys. Rev. C **89**, 045203 (2014).

[25] K. Bora and R. L. Jaffe, Double scattering contribution to $b_1(x, Q^2)$ in the deuteron, Phys. Rev. D **57**, 6906 (1998).

[26] J. Edelmann, G. Piller, and W. Weise, Deuteron spin structure functions at small Bjorken $x$, Phys. Rev. C **57**, 3392 (1998).

[27] J. Edelmann, G. Piller, and W. Weise, Polarized deuteron structure functions at small $x$, Z. Phys. A **357**, 129 (1997).

[28] L. Frankfurt, V. Guzey, and M. Strikman, Nuclear shadowing in inclusive and tagged deuteron structure functions and extraction of $F_2^p - F_2^n$ at small $x$ from electron-deuteron collider data, Mod. Phys. Lett. A **21**, 23 (2006).

[29] A. Bacchetta and P. J. Mulders, Deep inelastic leptoproduction of spin-one hadrons, Phys. Rev. D **62**, 114004 (2000).

[30] D. Boer, S. Cotogno, T. van Daal, P. J. Mulders, A. Signori, and Y.-J. Zhou, Gluon and Wilson loop TMDs for hadrons of spin $\leqslant 1$, J. High Energy Phys. 10 (2016) 013.

[31] S. Kumano, Parton distribution functions and fragmentation functions of spin-1 hadrons, Eur. Phys. J. A **60**, 205 (2024).

[32] J. Zhao, A. Bacchetta, S. Kumano, T. Liu, and Y.-J. Zhou, Semi-inclusive deep inelastic scattering off a tensor-polarized spin-1 target, J. High Energy Phys. 12 (2025) 067.

[33] S. Kumano and K. Kuroki, Tensor-polarized twist-3 parton distribution functions $f_{LT}(x)$ for the spin-1 deuteron by using twist-2 relations, Phys. Lett. B **875**, 140348 (2026).

[34] L. Trentadue and G. Veneziano, Fracture functions: An improved description of inclusive hard processes in QCD, Phys. Lett. B **323**, 201 (1994).

[35] J. C. Collins, Proof of factorization for diffractive hard scattering, Phys. Rev. D **57**, 3051 (1998); **61**, 019902 (2000).

[36] M. Anselmino, V. Barone, and A. Kotzinian, SIDIS in the target fragmentation region: Polarized and transverse momentum dependent fracture functions, Phys. Lett. B **699**, 108 (2011).

[37] L. L. Frankfurt and M. I. Strikman, High-energy phenomena, short range nuclear structure and QCD, Phys. Rep. **76**, 215 (1981).

[38] M. Strikman and C. Weiss, Electron-deuteron deep-inelastic scattering with spectator nucleon tagging and final-state interactions at intermediate $x$, Phys. Rev. C **97**, 035209 (2018).

[39] W. Cosyn and C. Weiss, Polarized electron-deuteron deep-inelastic scattering with spectator nucleon tagging, Phys. Rev. C **102**, 065204 (2020).

[40] N. Baillie *et al.* (CLAS), Measurement of the neutron $F_2$ structure function via spectator tagging with CLAS, Phys. Rev. Lett. **108**, 142001 (2012); **108**, 199902 (2012).

[41] S. Tkachenko *et al.* (CLAS), Measurement of the structure function of the nearly free neutron using spectator tagging in inelastic $^2\mathrm{H}(e, e' p_s)X$ scattering with CLAS, Phys. Rev. C **89**, 045206 (2014), [Addendum: Phys. Rev. C **90**, 059901 (2014)].

[42] W. Armstrong *et al.*, Partonic structure of light nuclei, arXiv:1708.00888.

[43] I. Albayrak *et al.*, Design, construction, and performance of the GEM based radial time projection chamber for the BONuS12 experiment with CLAS12, Nucl. Instrum. Methods A **1062**, 169190 (2024).

[44] A. V. Klimenko *et al.* (CLAS), Electron scattering from high-momentum neutrons in deuterium, Phys. Rev. C **73**, 035212 (2006).

[45] S. Gilad, O. Hen, L. B. Weinstein, S. A. Wood, *et al.*, In medium nucleon structure functions, SRC, and the EMC effect, JLAB-PR12-11-107 (2011), http://www.jlab.org/exp_prog/proposals/11/PR12-11-107.pdf.

[46] E. P. Segarra *et al.*, The CLAS12 backward angle neutron detector (BAND), Nucl. Instrum. Methods A **978**, 164356 (2020).

[47] A. Jentsch, Z. Tu, and C. Weiss, Deep-inelastic electron-deuteron scattering with spectator nucleon tagging at the future Electron Ion Collider: Extracting free nucleon structure, Phys. Rev. C **104**, 065205 (2021).

[48] R. Abdul Khalek *et al.*, Science requirements and detector concepts for the Electron-Ion Collider: EIC Yellow Report, Nucl. Phys. A **1026**, 122447 (2022).

[49] H. Huang, F. Méot, V. Ptitsyn, V. Ranjbar, and T. Roser, Polarization preservation of polarized deuteron beams in the electron ion collider at Brookhaven National Laboratory, Phys. Rev. Accel. Beams **23**, 021001 (2020).

[50] H. Huang, F. Méot, V. Ptitsyn, V. Ranjbar, and T. Roser, Feasibility of polarized deuteron beam in the EIC, in *12th International Particle Accelerator Conference* (IPAC, 2021).

[51] H. Huang, K. Hock, F. Meot, V. Ptitsyn, V. Ranjbar, V. Schoefer, and V. Morozov, Hadron polarization in the Electron Ion Collider, Proc. Sci. **PSTP2024**, 022 (2025).

[52] A. Kotzinian, New quark distributions and semi-inclusive electroproduction on the polarized nucleons, Nucl. Phys. B **441**, 234 (1995).

[53] M. Diehl and S. Sapeta, On the analysis of lepton scattering on longitudinally or transversely polarized protons, Eur. Phys. J. C **41**, 515 (2005).

[54] A. Bacchetta, M. Diehl, K. Goeke, A. Metz, P. J. Mulders, and M. Schlegel, Semi-inclusive deep inelastic scattering at small transverse momentum, J. High Energy Phys. 02 (2007) 093.

[55] S. Bastami *et al.*, Semi-inclusive deep inelastic scattering in Wandzura-Wilczek-type approximation, J. High Energy Phys. 06 (2019) 007.

[56] T. W. Donnelly, S. Jeschonnek, and J. W. Van Orden, General tensor structure for electron scattering in terms of invariant responses, Ann. Phys. **448**, 169174 (2023).

[57] W. Leidemann, E. L. Tomusiak, and H. Arenhövel, Inclusive deuteron electrodisintegration with polarized electrons and a polarized target, Phys. Rev. C **43**, 1022 (1991).

[58] A. Bacchetta, U. D'Alesio, M. Diehl, and C. A. Miller, Single-spin asymmetries: The Trento conventions, Phys. Rev. D **70**, 117504 (2004).

[59] F. G. Ledesma and M. Mewes, Spherical-harmonic tensors, Phys. Rev. Res. **2**, 043061 (2020).

[60] V. B. Berestetskii, E. M. Lifshitz, and L. P. Pitaevskii, *Quantum Electrodynamics*, Course of Theoretical Physics (Pergamon Press, Oxford, 1982), Vol. 4.

[61] G. Kramer, in *Electromagnetic Interactions of Hadrons*, Nuclear Physics Monographs, edited by A. Donnachie and G. Shaw (Springer, Berlin, 1978).

[62] N. Christ and T. D. Lee, Possible tests of $C_{\mathrm{st}}$ and $T_{\mathrm{st}}$ invariances in $l^{\pm} + N \to l^{\pm} + \Gamma$ and $A \to B + e^{+} + e^{-}$, Phys. Rev. **143**, 1310 (1966).

[63] A. Afanasev, M. Strikman, and C. Weiss, Transverse target spin asymmetry in inclusive DIS with two-photon exchange, Phys. Rev. D **77**, 014028 (2008).

[64] J.-Y. Kim and C. Weiss, Tensor-polarized parton density in the $N \to \Delta$ transition, Phys. Lett. B **870**, 139924 (2025).

[65] E. Leader, *Spin in Particle Physics* (Cambridge University Press, Cambridge, UK, 2001), Vol. 15.

[66] B. Keister and W. Polyzou, Relativistic Hamiltonian dynamics in nuclear and particle physics, Adv. Nucl. Phys. **20**, 225 (1991).

[67] W. R. Milner and R. G. Milner, Experimental scheme for polarizing boron nuclei, Phys. Rev. C **112**, 065204 (2025).

[68] S. Cotogno, C. Lorcé, P. Lowdon, and M. Morales, Covariant multipole expansion of local currents for massive states of any spin, Phys. Rev. D **101**, 056016 (2020).

[69] W. Cosyn and F. Vera, Spinor representations for fields with any spin: Lorentz tensor basis for operators and covariant multipole decomposition, J. High Energy Phys. 12 (2025) 068.